Characterize Oral-to-Blood Microbial DNA Translocation in Individuals with Cocaine Use Disorder

Douglas Johnson[1,2,3]*, Kamala Sundararaj[1]*, Suganya Subramanian[4], Yaxin Qiu[1,5], Iniyan Samuel[1,3], Da Cheng[1], Tabinda Salman[1], Zhenwu Luo[1], Sylvia Fitting[6], Larry Keen[7], Elizabeth Call[2], Abhiham Maddi[8], William Stoops[9], Alicia Hartley[10], John E. McKinnon[10], Zhuang Wan[1], Stefano Berto[1], Wei Jiang[1,2]

[1]Department of Pharmacology and Immunology, Medical University of South Carolina, Charleston, 29425, USA
[2]Ralph H. Johnson VA Health Care System, Charleston, 29403, USA
[3]University of South Carolina, Columbia, SC 29208, USA
[4]Neurogenomics Laboratory, Department of Neuroscience, Medical University of South Carolina, Charleston, SC 29425, USA
[5]Department of Psychology, College of Science, Northeastern University, Boston, MA 02115
[6]Department of Psychology & Neuroscience, University of North Carolina at Chapel Hill, Chapel Hill, NC 27599, USA
[7]Department of Psychology, College of Natural and Health Sciences, Virginia State University, VA 23806, USA
[8]Department of Advanced Specialty Sciences, College of Dental Medicine, Medical University of South Carolina, Charleston, 29425, USA
[9]Departments of Behavioral Science, Psychiatry and Psychology, Center on Drug and Alcohol Research, University of Kentucky, Lexington KY, 40536, USA
[10]Division of Infectious Diseases, Department of Medicine, Medical University of South Carolina, Charleston, SC 29425, USA

* Authors contributed equally
Corresponding author. Wei Jiang, 173 Ashley Ave. BSB208F, Charleston, SC, 29425; email: jianw@musc.edu.

Abstract

Background. Cocaine disrupts gut barriers in animal models, potentially enabling microbial translocation and inflammation in the periphery and central nervous system (CNS), but its direct role in inducing inflammation remains controversial. This study aimed to determine if the oral cavity is a source of circulating microbial DNA translocation in individuals with current cocaine use disorder (CUD).

Results. A cross-sectional case–control study was conducted, comparing CUD and demographically matched non-drug controls. Ten CUD (via smoking or vaping) and 24 controls provided paired saliva and blood samples. Microbial 16S rRNA V4 region was sequenced in isolated microbial DNA from saliva and plasma. Single-cell RNA sequencing (scRNAseq) was analyzed in human peripheral blood mononuclear cells. Saliva from CUD, but not plasma, exhibited reduced alpha diversity and altered beta diversity, characterized by enriched *Streptococcus* and depleted *Fusobacterium, Neisseria,* and other taxa relative to controls. Controls exhibited low to undetectable microbial translocation in plasma. By contrast, plasma *Streptococcus* and several S. species displayed CUD-specific oral enrichment and evidence of translocation into the bloodstream. *In vitro*, cocaine selectively enhanced *S. parasanguinis* growth, consistent with CUD-enriched oral pathobionts and translocation into circulation *in vivo*. *S. parasanguinis*, but not cocaine alone, induced IL-1β and TNF-α production in human primary monocytes. scRNAseq further revealed innate immune activation, impaired T cell function, and heightened susceptibility to infection in CUD.

Conclusions. This is the first study demonstrating that CUD via smoking or snorting exhibited oral microbial dysbiosis and selective oral-to-blood microbial translocation in vivo. These findings suggest that a compromised oral-to-blood barrier, rather than cocaine itself, promotes immune perturbations in CUD.

Key words: cocaine use disorder, oral microbiome, oral-to-blood microbial DNA translocation

INTRODUCTION

Cocaine, used by 5 million people in the U.S. in 2023 [1], is associated with systemic inflammation, immunodeficiency, increased susceptibility to infections, and central nervous system (CNS) abnormalities, including reduced frontal lobe grey matter and impaired cognitive function [2, 3]. The mechanisms underlying these inflammatory and immune perturbations are not fully understood.

The human oral microbiome is essential in maintaining oral health by preserving homeostasis through regulating oral immunity and metabolism [4]. Recent studies suggest that non-intravenous cocaine use causes oral microbiome dysbiosis, characterized by an enrichment of opportunistic pathogens and a reduction in beneficial commensal microorganisms [5, 6]. Oral bacterial translocation to the blood has been reported in healthy individuals after tooth brushing [7-9]. Disruption of the microbial balance may contribute to the progression of oral diseases, including periodontitis and dental caries, with implications in systemic conditions. Several bacteria translocate from the oral cavity to the circulation and have been linked to cardiovascular diseases, pre-term birth, rheumatoid arthritis, and Alzheimer's Disease (e.g., *Streptococcus mutans, Porphyromonas gingivalis*) [10-15]. Proinflammatory microbial translocation contributes to local inflammation and facilitates the entry of bacterial products into the circulation, thereby contributing to systemic inflammation via pattern recognition receptors (PRRs), such as toll-like receptors (TLRs) [16-18].

Chronic cocaine use has been associated with heightened systemic and CNS inflammation [19-21]. Cocaine itself exhibits both immunosuppressive and immunostimulatory effects on host cells from *in vitro* [22, 23] and *in vivo* studies [24-27]. Given the ability of microbes or microbial products to enter the bloodstream following a comprised oral barrier, the potential translocation of oral

microbes or their byproducts may play an indirect role in chronic cocaine use-associated persistent systemic inflammation and complications.

In this study, we report that individuals with current cocaine use disorder (CUD) via smoking or snorting exhibited altered oral microbiome by enriching cocaine-specific opportunistic pathogens (pathobionts) and depleting beneficial commensals, as well as evidence of oral-to-blood selective microbial translocation.

METHOD

Participants

Participants were recruited in Charleston, SC, USA. The non-drug controls were recruited via community advertisements to match the age and sex of CUD. Ten CUD and twenty-four controls who refrained from any drug use for at least one year, aged from 18 to 55 years, were enrolled. The Medical University of South Carolina (MUSC) Institutional Review Board approved this study; all participants provided written informed consent. Participants of CUD were through smoking or snorting. History or current diagnosis of psychiatric, neurological or neurodevelopmental disorders, traumatic brain injury, or recent antibiotic or probiotic usage was excluded. CUD was diagnosed through the Diagnostic and Statistical Manual of Mental Disorders, 5th edition (DSM-V), without the report of the current use of the other four drugs confirmed through chart reviews and urine 5-drug tests (Cocaine, Marijuana, Opiates, Methamphetamines, and Amphetamines, UTest Drug Testing, Framingham, Massachusetts), as described in our previous study [28]. Clinical characteristics of study participants are shown in Table 1.

Microbiome analysis

The detailed microbial 16S rRNA sequencing method was shown in our previous studies [28-30]. Briefly, unstimulated saliva was collected; bacterial DNA was extracted from saliva using the QIAamp DNA Microbiome Kit (Qiagen, Germantown, MD, USA). Plasma microbial DNA was isolated from 400 μL samples using the QIAamp UCP Pathogen Mini Kit (Qiagen). Subsequently, the bacterial 16S rRNA V4 variable region was sequenced at the Microbial Analysis, Resources, and Services, University of Connecticut (Storrs, CT).

Bacterial growth curve assay

S. parasanguinis strain F0449 (HM-808; BEI Resources, Manassas, VA) was cultured overnight in Trypticase Soy Broth (TSB; Sigma-Aldrich, St. Louis, MO) at 37 °C, diluted to OD600 = 0.1 in

ZMB1 chemically defined medium [31], and supplemented with 100 mM glucose. Bacterial cultures were treated with cocaine hydrochloride (5 and 50 µg/mL; Sigma-Aldrich) or medium control. The lower dose of cocaine reflects upper-range physiological blood levels [50]. Growth in triplicate was monitored by OD600 over 20 h at 37°C [32]. Additional strains included *S. thermophilus* (BAA-491; ATCC, Manassas, VA), *S. sanguinis* (DSS-10; ATCC), and *S. australis* (DSM 15627; DSMZ, Braunschweig, Germany).

Pro-inflammatory cytokine production in response to *S. parasanguinis*

Frozen PBMCs from four healthy donors were thawed with DNase I (20 µg/mL) [28]. Heat-inactivated *S. parasanguinis* (1.25 × 10^6/mL, 65 °C for 30 min) was added with or without cocaine (5 µg/mL) in the presence of GolgiStop and GolgiPlug (1 µL/mL) for 6 h. Monocyte CD14 and intracellular cytokines (Biolegend, Los Angeles, CA) were measured by flow cytometry and analyzed with FlowJo.

Single-cell RNA sequencing (scRNAseq)

scRNAseq was performed on PBMCs from 2 CUD and 2 age-matched controls; all were white males (Singulomics Corporation, Bronx, YN). Cells were captured via 10x Genomics Chromium-X GEM-X v4, with 3′ libraries sequenced on Illumina NovaSeq X Plus (~500 million PE150 reads/sample). Reads were processed with Cell Ranger v9.0 (GRCh38-2024-A reference, including introns) to generate gene–cell matrices; ambient RNA was removed via CellBender v0.2.0, and alignment to hg38 (gencode.v42) followed. Data integration (Seurat v5.0.0) included cell cycle analysis (CellCycleScoring), with cells retained if they had <100,000 UMIs, <20% mitochondrial reads, and no doublets (scDblFinder v1.12.0), yielding 20,017 features and 5,659 cells. Normalization, integration, and variable gene selection used SCTransform (30 PCs, resolution 0.6, UMAP); batch effects were corrected with Harmony v0.1.1. Post-RBC removal,

reclustering identified 15 clusters. Cell types were annotated via FindAllMarkers, RunAzimuth, and canonical markers. Differential cell abundance was assessed with scProportionTest; DEGs (FDR < 0.05, |log2FC| > 0.3) were identified using LIBRA v1.0.0. Cell-cell communication was analyzed with CellChat v2.1.2; DEG functional annotation used scToppR v0.99.1 and clusterProfiler v4.12.2. Pathways were selected via Mann–Whitney U tests (false discovery rate [FDR] < 0.01).

Microbiome CpG Index

For each sample, metagenomic reads were mapped to phylum-specific reference genomes using Bowtie2 (v2.4.5). The CpG index was computed as the mean number of stimulatory hexamers (RRCGYY, where R = A/G, Y = C/T) minus the mean number of inhibitory hexamers (NCCGNN and NNCGRN), normalized per kilobase of mapped sequence, following the method described by Lundberg et al. [33]. Phylum-level CpG indices were aggregated by averaging across taxa within each phylum, proportional to their abundance.

Statistical Analysis

OTU counts were normalized to relative abundances, and taxa were aggregated at phylum, class, order, family, genus, and species levels. To evaluate for a significant difference in composition (i.e., whether the groups occupy distinct regions in multivariate space, as hinted by the plot), a permutational multivariate analysis of variance (PERMANOVA) was conducted on the full Bray-Curtis distance matrix. Group differences in abundances were assessed using the non-parametric Mann–Whitney U test in QIIME 1, with FDR correction. α-diversity within samples was calculated using the phyloseq package in R and compared by the Wilcoxon rank sum test. Differences in overall microbiome composition between groups were evaluated by permutational multivariate analysis of variance (Adonis function, vegan package in R), with P values adjusted by the

Benjamini–Hochberg FDR method. Statistical significance was defined as $P < 0.05$. Analyses were performed using GraphPad Prism (version 10.4.1, GraphPad Software, Boston, MA, USA).

RESULTS

CUD-associated microbiome dysbiosis in saliva but not in plasma

In saliva, α-diversity (Simpson Index) was significantly reduced at the phylum ($p < 0.0001$), genus ($p < 0.0001$), and species levels ($p < 0.05$) (Figure 1A–1C), indicating decreased oral bacterial richness in CUD. In plasma, no difference of α-diversity was determined between the two study groups ($P > 0.05$). β-diversity (Bray–Curtis PCoA) revealed significant group differences in saliva at all levels, as well as plasma at the genus level ($p = 0.02$) but not at the phylum or species level ($p > 0.05$) (Figure 1D–1F). These findings demonstrate that CUD significantly disrupts the oral microbial community, with minimal changes in circulating microbial diversity.

Relative abundance of bacteria in saliva and plasma

We next assessed the enrichment of taxa in CUD versus controls. Overall, more taxa were detected with low abundance in the plasma compared to saliva at each levels, suggesting plasma microbial translocation from various sources besides the oral cavity (Figure 2A-2B, supplemental Figures 1-2). At the phylum level (Fold changes in CUD versus controls, supplemental Figure 1A), CUD saliva was enriched for *Firmicutes* and *Actinobacteria* and depleted of *Fusobacteria*, *Bacteroidetes,* and *Proteobacteria*, whereas CUD plasma showed higher *Proteobacteria, Actinobacteria, Firmicutes,* and lower *Nitrospirae,* and others. Notably, heatmap analysis revealed *Streptococcus* as the predominant oral genus translocated into plasma in CUD but not controls, despite being orally present in both groups (Figure 2A; supplemental Figures 1B and 2A). At the genus level, CUD saliva was enriched for *Streptococcus* and depleted of *Fusobacteria*, *Granulicatella, Heamophilus, Leptotrichia, Neisseria, Porhpyromonas,* and *Proteobacteria*, whereas CUD plasma showed higher *Streptococcus* and *Neisseria* and lower *Leptotrichia* and *Porphyromonas* (Figure 2A). At the species level (Figure 2B, supplemental Figure 2B), *Streptococcus* profiling showed higher *S. species* (e.g., *S. australis*, *S. parasanguinis*, *S. vestibutaris,* and *S. thermophilus*) and *Veillonella dispar*, with lower *Neisseria mucosa, N. cinerea,*

N. flavescens, Prevotella melaninogenica, Granulicatella adiacens, Actinobacillus porcinus, and *Haemophilus parainfluenzae* in saliva of CUD. Among the four S. species increased in saliva of CUD, *S. australis* and *S. parasanguinis* increased in plasma of CUD versus controls.

Increased abundance of saliva Gram-positive bacteria in CUD versus controls

We next evalute the enrichment of Gram-positive and negative bacteria (Figure 2C), and found that overall more Gram-positive versus Gram-negative in both saliva and plasma from both groups; saliva but not plasma from CUD exhibited further increased abundance of Gram-positive bacteria compared to controls. These findings suggest a relatively consistent oral-to-blood microbial shift in CUD, whereas in controls, the blood microbiome appears to derive more from other sources (e.g., gut) besides the oral cavity.

Oral-to-blood microbiome DNA translocation

To futher evaluate oral-to-blood microbial translocation, we analyzed shared genera and species in both sampling sites and compared between the two study groups (Figures 3A-3B, median ± 95% CI). The overall microbial translocation in plasma was significantly low in controls verus CUD, consistent with the integration of barriers in healthy individuals but no in CUD. Notably, CUD exhibited mainly increased *Streptococcus* in both sites, especially in the plasma, compared to controls. At the species level (Figure 3B), *S. sanguinis*, *S. australis*, and *S. parasanguinis* were enriched in both saliva and plasma of CUD, consistent with oral-to-blood translocation. In contrast, controls exhibited higher abundances of *Neisseria* and *Haemophilus*, hallmarks of a balanced oral microbiome [34], while CUD showed a shift toward opportunistic pathogenic taxa.

Focusing on oral-associated taxa [35], *Streptococcus* and *Actinomyces* were increased in both saliva and plasma of CUD (Figure 2A and Figure 3A). The plasma-to-saliva ratio of *Streptococcus*, but not *Actinomyces*, was elevated in CUD compared with controls (Figure 3C), suggesting

differential translocation potential. In controls, *Streptococcus*, *Neisseria*, *Haemophilus*, and *Rothia* remained largely restricted to saliva and rarely detected in plasma. These findings indicate selective oral-to-blood microbial DNA translocation in CUD, reflecting compromised barrier function and dysbiosis.

Cocaine promotes the growth of *S. parasanguinis,* a proinflammatory microbiota, *in vitro*

Given the enrichment of *Streptococcus* species in the saliva and plasma of CUD, we assessed whether cocaine directly affects their growth. Notably, cocaine significantly enhanced *S. parasanguinis* growth, whereas *S. australis*, *S. thermophilus*, and *S. sanguinis* were unaffected (Figure 4A). No difference was observed between the two cocaine concentrations (Supplemental Figure 3), and the lower one selected corresponded to the physiological level found in cocaine users [36]. These findings indicate that cocaine selectively promotes *S. parasanguinis* growth, potentially explaining its enrichment in CUD.

Host cell interactions with various microbes lead to the production of pro-inflammatory cytokines [16]. To verify whether *S. parasanguinis* exhibits proinflammatory activity, we cultured PBMCs with heat-inactivated *S. parasanguinis* and found a noticeable increase in the production of TNF-α and IL-1β (Figure 4B). However, cocaine did not impact the cytokine production (Figure 4B). These findings suggest that cocaine may promote systemic inflammation indirectly by enriching and translocating proinflammatory microbiome elements, rather than acting as a direct inducer.

Reduced CpG index in oral microbiome phyla of CUD

The CpG index, measuring bacterial DNA's net immunostimulatory potential, was calculated for the five dominant phyla (Firmicutes, Bacteroidetes, Proteobacteria, Actinobacteria, Fusobacteria) in each sample (Figures 5A-5B). All phyla had positive CpG indices (indicating oral microbiome

immunostimulatory potential), with plasma microbiome showing unexpectedly higher CpG indices than saliva. Aggregate phylum-level CpG indices were significantly lower in CUD than controls. Oral phyla of controls (Firmicutes, Bacteroidota, Actinobacteriota, Proteobacteria) had CpG indices clustering near the neutral range indicating relative genomic stability, while CUD had significantly reduced CpG indices indicating oral microbial CpG suppression. The CpG index reduction was most pronounced in *Firmicutes* and *Actinobacteriota*, phyla enriched in opportunistic taxa (e.g., *Streptococcus, Actinomyces*) with oral-to-blood translocation evidence. This suggests CUD-associated oral dysbiosis favors microbes with greater CpG depletion linked to host–pathogen interactions and immune evasion, indicating CUD alters oral microbiome taxonomic composition and genomic CpG content.

scRNAseq profiling reveals distinct circulating immune perturbations in CUD versus controls

scRNAseq of PBMCs identified 12 immune populations (e.g., CD4+ and CD8+ T cell subsets, CD14+/CD16+ monocytes, DCs, B cells, NK cells, platelets) in CUD and controls (Figure 6A-6E). CUD showed immune composition shifts: increased NK cells, total B cells, and platelets; reduced CD4+ and CD8+ T cell subsets and naive B cells (Figure 6C-6D; supplemental Figure 4). Differential gene expression (DGE) was most prominent in CD8+ effector T cells (1,504 DEGs), CD4+ memory T cells (625), CD14+ monocytes (570), and DCs (386) (Figure 6D). Most DEGs were upregulated, including genes related to immune activation and function, such as RPS4Y1, UTY, and DDX3Y, in lymphocytes and monocytes but not platelets, NRGN (CD4+ naive T cells, adaptive neuroimmune response), and HBA1 (multiple cells, oxidative stress compensation) (Figure 6E and 7A). Downregulated DEGs included RGPD2 (broad cell types, cellular processes), NEBL (monocytes, cytoskeletal function), and CCL3L3, FCER1A, and CD8A (monocytes, innate immune suppression) (Figure 6E and 7A).

Pathway analysis revealed CUD upregulated innate immunity (NOD-like receptor signaling, NK activation, antigen processing) and pathogen response pathways, but downregulated adaptive immunity (TCR signaling, Th cell differentiation, chemokine signaling) (Figure 7B). Cell-cell communication in CUD showed reduced network density and connectivity (especially T cells and monocytes) compared to controls (Figure 7C), indicating impaired intercellular coordination. These findings support CUD-driven innate immune activation, adaptive immune suppression, and immune dysregulation, likely linked to microbial translocation (e.g., S. parasanguinis) rather than cocaine directly.

DISCUSSION

In this study, CUD was characterized by oral microbial dysbiosis, reflecting the expansion of opportunistic oral pathogens (e.g., *Streptococcus spp*.). While several species were consistently enriched in both saliva and plasma when comparing CUD versus controls, the data suggest that plasma microbial translocation in CUD originates at least partially from the oral cavity. Controls exhibited significantly low to undetectable levels of microbial translocation. However, CUD-specific oral-to-blood translocation may be diluted within the broader physiological background of microbial translocation from other compartments, such as the gut, which was evident in controls.

Chronic cocaine use is strongly associated with oral health deterioration, including periodontitis [37]. Reduced salivary flow, a common consequence of cocaine use, diminishes pathogen clearance and contributes to oral dysbiosis [38]. Cocaine also exerts immunomodulatory effects that favor colonization by opportunistic pathogens [37], increasing susceptibility to infections [39, 40]. Studies conflict on the direct impact of cocaine on anti- or pro-inflammatory responses, ranging from enhanced proinflammatory responses to inhibition of myeloid cell activation [22-27]. In humans, acute cocaine administration suppresses peripheral inflammation, reducing monocytic TNF-α and IL-6 production [41]. By contrast, chronic cocaine use is linked to dysregulated systemic inflammation [42] and neuroinflammation, characterized by microglial activation and neuropathology in both animal models and humans [43, 44]. These effects may arise from direct neurotoxicity on glial cells [43] as well as indirect mechanisms. Prolonged use disrupts mucosal barrier integrity and alters microbiota composition, promoting microbial translocation into circulation. While some studies suggest cocaine may impair epithelial barriers directly [19, 45], others indicate that barrier disruption is not solely cocaine-mediated [22]. Instead, microbiota-driven dysbiosis is likely to contributes to barrier dysfunction. Thus, we propose that microbial shifts, rather than cocaine itself, drive host immune activation, and persistent inflammation.

Cocaine use induces a compromised barrier and alters gut microbiomes in previous human and animal studies [19, 46, 47]. Although most microbiome research has focused on the gut, our data show that in CUD, the plasma microbiome partially mirrors that of saliva. These results implicate the oral cavity exposed during smoking or snorting as a source of microbial translocation into the bloodstream in CUD.

The CpG index, a measure of the immunostimulatory potential of bacterial DNA, was calculated at the phylum level using representative reference genomes for dominant taxa within each phylum, weighted by their relative abundance in the metagenome. Controls displayed a wider range of CpG values, characterized by a higher median index and greater variability, consistent with a more diverse and potentially immunostimulatory microbial milieu. In contrast, CUD exhibited clustered lower CpG values and fewer high-index outliers, reflecting a shift toward reduced inflammatory potential. Collectively, these findings support the hypothesis that cocaine use-associated impairment of oral barriers, rather than a cocaine-induced shift in the oral microbiome toward a proinflammatory community, constitutes a central pathogenic mechanism enabling oral microbiome translocation.

This is the first human study to provide evidence of such a compromised barrier in CUD, marking a significant step in understanding the systemic consequences of CUD via oral health disruptions. However, we cannot entirely exclude the possibility that oral microbiome DNA translocates to the blood via the gut. Nonetheless, multiple pieces of evidence from other colleagues support the translocation of oral-to-brain rather than oral-to-gut in CUD: 1) human studies using paired samples from different sites, revealed that the predominant colonization of *Streptococcus* species; for example, *S. parasanguinis* exhibits 100-1000-fold higher copies per ng of microbial DNA in the saliva versus stool [35, 48]; and 2) clinical evidence of bacteria translocation from the oral cavity to the system contributing to the development of preterm birth, stroke, and metabolic

disorders [12, 49, 50]. Our results highlight that chronic cocaine exposure via smoking or snorting destabilizes the oral ecosystem, enabling persistent oral-to-blood translocation, which may contribute to CUD-associated complications, including elevated innate immunity and systemic inflammation, immune perturbations, and susceptibility to infections.

Oral *Streptococci* have a dual nature. While typically harmless (or even protective) in the oral cavity, if they or their byproducts gain access to systemic body sites, they can cause disease. For example, many oral *Streptococci* express surface proteins that bind extracellular matrix components (collagen, fibrin) and platelet receptors, facilitating their attachment at sites like damaged endocardium or blood vessels and contributing to systemic diseases [51-54]. However, these cases occur more frequently in immunocompromised individuals. Certain oral *Streptococcus* strains possess immune-evasive and proinflammatory properties that facilitate both colonization and pathogenicity. Traits such as adherence, biofilm formation, and immune modulation, while critical for oral biofilm stability, also enable invasive potential when bacteria are displaced [55, 56]. Chronic oral dysbiosis, as in periodontitis, exacerbates this risk by increasing bacterial burden and weakening mucosal integrity. Periodontitis-associated *Streptococcus* species can persist within inflamed gingival tissues, provoking sustained systemic immune activation or intermittently translocating into circulation [57, 58]. Thus, *Streptococcus* species play a context-dependent role, as essential contributors to oral homeostasis under balanced conditions, but potential drivers of systemic inflammation and infection when homeostasis is disrupted. Their capacity to modulate immune responses locally and systemically underscores their importance in linking oral health to overall health.

Several mechanisms account for cocaine promoting *S. parasanguinis* overgrowth. Cocaine-induced alterations in the oral environment, including xerostomia and reduced pH, favor *Streptococcal* adhesion and plaque formation. Viridans *Streptococci*, such as *S. parasanguinis*, express virulence factors like the serine-rich adhesin Fap1, which enhance attachment and

extracellular polysaccharide production within biofilms [59]. Another possibility is that *S. parasanguinis* might metabolize cocaine or its derivatives to gain a growth advantage. Notably, certain environmental bacteria produce a cocaine esterase (CocE) that hydrolyzes cocaine into benzoate and ecgonine methyl ester, allowing those microbes to use cocaine as a carbon and energy source [60]. While this enzymatic activity remains understudied involving *S. parasanguinis*, exploring whether oral *Streptococci* harbor similar cocaine-metabolizing enzymes is a compelling area for future research. Overall, our findings underscore that CUD-associated oral microbiome shifts, particularly the overabundance of proinflammatory *Streptococcus* species, have significant implications for host health. Further investigation is warranted to establish a causal relationship between these microbial shifts, biofilm formation, and systemic host immune responses to mitigate the health risks in CUD.

In saliva, opportunistic taxa such as *Streptococcus* were enriched, whereas commensals *Neisseria, Prevotella,* and *Haemophilus* were depleted, consistent with oral dysbiosis. Among these changes in saliva, several were also observed in plasma. The detection of specific *Streptococcus* species in both saliva and plasma suggests oral-to-blood microbial DNA translocation in CUD (Figure 3B). Notably, *Neisseria* was a highly enriched genus in control saliva (controls versus CUD, Figures 2A and 3A), whereas *N. subflava* was detected exclusively in the blood of CUD but low in controls (Figure 3B); *F. periodonticum, F. nucleatum* and *R. aeria* were identified only in the blood of CUD (Figure 3B), consistent with a compromised oral–blood barrier. Despite site-specific differences, overall microbial enrichment patterns were similar between groups, suggesting selective and microbiome-specific translocation that warrants further investigation.

It is important to note that our findings do not indicate the translocation of whole live bacteria in CUD, as this could result in septicemia [61]; no clinical infection was observed in all study

participants during the study visit. Instead, we propose that bacterial byproducts, such as DNA fragments, bacterial cell wall products (i.e., LPS and PGN), and other microbial antigens (i.e., microbial metabolites), show different abilities to induce proinflammatory cytokine production [30] via entering the bloodstream persistently and contributing to chronic systemic inflammation [62, 63], deserving further investigations. This perspective aligns with CUD-mediated systemic inflammation and pathology indirectly via oral-to-blood microbial translocation or entering through the lymphatic system [64].

Building on prior reports of immune dysregulation and immunodeficiency, impaired adaptive immunity, and elevated rates of cardiovascular, infectious, and neuropsychiatric comorbidities in CUD [42-44, 65], scRNA-seq revealed heightened activation of innate immune pathways (e.g., NOD-like receptor signaling, NK cell cytotoxicity) and increased infection susceptibility, accompanied by broad suppression of T-cell receptor signaling in CUD, indicating innate hyperactivation coupled with impaired adaptive immunity. Predicted disruption of cell–cell communication networks further indicated compromised immune coordination.

While our study is the first to illuminate the potential for oral-to-blood microbial translocation in CUD, it is not without limitations. 16S rRNA V4 sequencing, employed herein, lacks precise species-level resolution, metagenomic shotgun sequencing or full-length 16S RNA sequencing represents a more advanced approach for future investigations. Notably, *in vitro* experiments demonstrating cocaine-induced growth of *S. parasanguinis* align with our *in vivo* human microbiome findings at the species level, mitigating this limitation in part. Additionally, the small sample size of scRNA-seq data restricts the scope of conclusions we can draw. To fully elucidate the temporal dynamics of microbial translocation and its downstream health impacts in CUD, causal and longitudinal studies are warranted.

CONCLUSIONS

This study demonstrates that oral microbiome dysbiosis and impaired oral barrier integrity in COC enable persistent oral-to-blood microbial translocation. The selective enrichment of *S. parasanguinis* growth suggests cocaine promotes the expansion of pathobionts with potential systemic sequelae. Single-cell transcriptomic analyses further revealed a signature of innate immune activation, heightened infection susceptibility, and compromised T-cell-mediated adaptive immune responses, supporting a model wherein translocated microbial products sustain immune dysregulation. Notably, this is the first *in vivo* study to link CUD-associated oral barrier dysfunction to systemic immune perturbations. These findings highlight the oral cavity as a key yet underappreciated driver of systemic immune dysfunctions in CUD, bridging local microbial alterations to broader systemic disturbances. Future research should investigate whether targeted microbiome interventions can restore oral barrier function, rebalance host–microbe crosstalk, and ultimately alleviate CUD-associated systemic pathogenesis.

AUTHOR CONTRIBUTIONS

D.J., K.S. I.S., A.H., and Z.L., performed experiments. D.J. and Y.Q. wrote the manuscript. Z.W., W. X., D.J., S.S., and W.J. analyzed data. E.C., D. C., L.K., J.E.M., W.S., T.S., S.B., S.F., A.M., and W.J. revised the manuscript.

ACKOWLEDGEMENTS AND FUNDINGS

This work was supported by grants from the National Institutes on Drug Abuse R01DA059854 (Jiang), R01DA059538 (Jiang), R01DA055523 (Fitting & Jiang), 2R15DA052886-02 (Keen), and by the Odyssey Pre-doctoral Fellowship from the Medical University of South Carolina College of Graduate Studies, the CNDD Genomics and Bioinformatics Core at MUSC (NIH grant P20GM148302), and by the Biorepository & Tissue Analysis Shared Resource, Hollings Cancer Center, Medical University of South Carolina (P30 CA138313).

HUMAN ETHICS AND CONSENT

The Medical University of South Carolina (MUSC) Institutional Review Board approved this study; all participants provided written informed consent.

Clinical trial number: not applicable.

DECLARATION OF INTERESTS. None.

DATA AVAILABILITY STATEMENT

The NCBI Gene Expression Omnibus (GSE304577) accession number for the single-cell RNA-seq data is available. Single-cell data is available through a shiny app: https://bioinformatics-musc.shinyapps.io/JiangLab_COCAINE_study/. Custom R codes and data to support the analysis, visualizations, and functional enrichments are available at https://github.com/BioinformaticsMUSC/JiangLab_CUDAINEproject.

Table 1

Characteristics	Controls	CUD	P value
N (M/F)	24 (19/6)	10 (3/7)	
Age (mean y, SD)	35.6 (10.3)	40.3 (13.8)	NS[a]
Race (n, %)			NS[c]
White	9 (38)	7 (70)	
Black	5 (21)	2 (20)	
Others	10 (41)	1 (10)	

[a]Student's t test
[c]Exact test

Figure legends

Figure 1. Oral but not blood microbial dysbiosis in CUD. (A-C) Saliva and plasma microbiome α-diversity (mean ± SD, non-parametric MannWhitney tests) and (D-F) β-diversity in CUD and controls. **** $p<0.0001$, NS: $P > 0.05$. Each point represents an individual sample, with horizontal lines indicating group means. A permutational multivariate analysis of variance (PERMANOVA) was applied to β-diversity on the full Bray-Curtis distance matrix.

Figure 2. Comparative analysis of microbial abundance in saliva and plasma samples from CUD versus controls. (A-B) Heatmap (median relative abundance, log2) and dot plots (median relative abundance, log2 or percentages) analysis of shared microbial genera and species in saliva and plasma samples. Shared taxa in saliva were selected from the top-enriched genera or species in any group. (C) Relative abundance of Gram-positive and Gram-negative genera in saliva and plasma. Mean ± SEM.

Figure 3. Oral-to-blood microbiome consistency. (A-B) Relative abundance of bacterial genera (A) and species (B) in saliva and plasma samples of CUD and controls, emphasizing

potential oral-to-blood tranlocation. Data is shown as median ± 95% CI; taxa was selected for detecting in both sites. (C) Plasma-to-saliva ratios (log2) of *Streptococcus* and *Actinomyces* between the two study groups.

Figure 4. Cocaine promotes the growth of proinflammatory species*, S. parasanguinis in vitro.* (A) Four *Streptococcus* species were cultured with cocaine at 5 μg/mL *in vitro*, supplemented with glucose (50 mM) in ZMB1 media. Bacterial growth curve was assessed by Optical density (OD600). (B) PBMCs isolated from four healthy donors were stimulated with *S. parasanguinis* (SP), cocaine, or a combination of SP and cocaine. The production of pro-inflammatory cytokines TNF-α and IL-1β was measured using ELISA. Data are presented as mean ± SD, and statistical significance is indicated as follows: **$p < 0.01$; ****$p < 0.0001$.

Figure 5. Distribution of CpG indices at the phylum level for CUD (red) and control (blue) groups. (A) CpG indices in each genera from saliva and plasma. (B) CpG indix comparisons in the two study groups. Comparisons of CpG index distributions in CUD were lower than controls. Data are presented as boxplots showing median, interquartile range (IQR), and individual sample distributions. Phylum-specific analyses revealed the most pronounced reductions in Firmicutes ($p = 0.002$) and Bacteroidetes ($p = 0.004$) in CUD, which may contribute to altered immune responses in the oral cavity. No significant correlations were found between CpG index and cocaine use duration or frequency (Spearman's $\rho < 0.2$, $p > 0.1$).

Figure 6. scRNAseq of PBMCs from CUD and controls. (A) Workflow schematic of scRNA-seq analysis. (B) UMAP plots showing distinct clustering of immune cell populations in CUD versus controls. (C) Differential cell-type composition, with significant shifts in NK, B cells, monocytes, and platelets, alongside stacked bar graphs of relative proportions. (D) Bar plots of DEGs across immune cell populations, showing both total numbers and the numbers of up- and

down-regulated DEGs. CD8+ effector T cells, monocytes, and memory CD4+ T cells showed the most significant transcriptional changes. (E) Heatmap of representative DEGs by cell type, with red indicating upregulation and blue indicating downregulation, based on the top means of 80 up- and 80 down-regulated genes in CUD versus controls in any cell type.

Figure 7. Differential gene expression, pathways, and cell–cell communication in CUD versus controls. (A) Volcano plots of representative immune subsets show significantly upregulated (red, ratio of CUD versus controls) and downregulated (blue, ratio of CUD versus controls) genes in CUD versus controls, with top markers labeled. Above the grey line indicates an adjusted p-value < 0.01. (B) Pathway enrichment analysis highlights upregulation of NK activation, antigen presentation, NOD-like signaling, and infection-related pathways, alongside downregulation of TCR signaling, Th differentiation, chemokine signaling, and PD-1 checkpoint pathways. (C) Chord diagrams illustrate predicted ligand–receptor interactions, with controls showing balanced networks and CUD exhibiting altered connectivity and disrupted immune communication.

Supplemental Figure 1. Box plots depict log2 fold changes in bacterial taxa between groups at the (A) phylum and (B) genus levels. Genus column median > 0.007 was selected.

Supplemental Figure 2. **Taxonomic composition of saliva and plasma microbiomes in CUD and controls.** Stacked bar plots of bacterial genera (A) and species (B) show the mean enrichment of oral- and plasma-associated taxa.

Supplemental Figure 3. **Effects of cocaine on *S. parasanguinis* growth.** Optical density (OD600) measurements of *S. parasanguinis* cultured under various conditions, including

media alone, media supplemented with cocaine (5 μg/mL and 50 μg/mL), and supplemented with glucose (100 mM).

Supplemental Figure 4. **Altered cell–cell communication and gene expression in PBMCs from CUD versus controls.** (A) Heatmaps show predicted incoming and outgoing signaling patterns across immune subsets, with CUD samples displaying distinct shifts in ligand–receptor signaling strength compared to controls. (B) Boxplots highlight representative DEGs, including *TSC22D3*, *CD83*, *CD300A*, *HLA-C*, *CAVIN2*, *GRAP2*, *EBX3*, *IFI16*, *DAP*, *LAIR2*, *FMN1*, *EPSTI1*, *RHOB*, *F2R*, *CDK11A*, *CD226*, *HLA-DQB1*, and *CEBPD*, demonstrating significant transcriptional alterations in CUD.

References

1. Administration SAaMHS: **Key substance use and mental health indicators in the United States: Results from the 2023 National Survey on Drug Use and Health (HHS Publication No. PEP24-07-021, NSDUH Series H-59)**. *Center for Behavioral Health Statistics and Quality, Substance Abuse and Mental Health Services Administration* 2024.
2. Buttner A, Mall G, Penning R, Sachs H, Weis S: **The neuropathology of cocaine abuse**. *Leg Med (Tokyo)* 2003, **5 Suppl 1**:S240-242.
3. Beheshti I: **Cocaine Destroys Gray Matter Brain Cells and Accelerates Brain Aging**. *Biology (Basel)* 2023, **12**(5).
4. Baker JL, Mark Welch JL, Kauffman KM, McLean JS, He X: **The oral microbiome: diversity, biogeography and human health**. *Nature Reviews Microbiology* 2024, **22**(2):89-104.
5. Gerace E, Baldi S, Salimova M, Di Gloria L, Curini L, Cimino V, Nannini G, Russo E, Pallecchi M, Ramazzotti M *et al*: **Oral and fecal microbiota perturbance in cocaine users: Can rTMS-induced cocaine abstinence support eubiosis restoration?** *iScience* 2023:106627.
6. Fu X, Cheng D, Luo Z, Wagner A, Fitting S, Cong X, Xu W, Maas K, Wan Z, Zhu J *et al*: **Oral Enrichment of Streptococcus and its Role in Systemic Inflammation Related to Monocyte Activation in Humans with Cocaine Use Disorder**. *Journal of Neuroimmune Pharmacology* 2022, **17**(1):305-317.
7. Bahrani-Mougeot FK, Paster BJ, Coleman S, Ashar J, Barbuto S, Lockhart PB: **Diverse and novel oral bacterial species in blood following dental procedures**. *Journal of clinical microbiology* 2008, **46**(6):2129-2132.
8. Lockhart PB, Brennan MT, Sasser HC, Fox PC, Paster BJ, Bahrani-Mougeot FK: **Bacteremia associated with toothbrushing and dental extraction**. *Circulation* 2008, **117**(24):3118-3125.
9. Kaplan EL: **Letter by Kaplan regarding article, "Bacteremia associated with toothbrushing and dental extraction"**. *Circulation* 2009, **119**(2):e13; author reply e14.
10. Li Y, Zhu M, Liu Y, Luo B, Cui J, Huang L, Chen K, Liu Y: **The oral microbiota and cardiometabolic health: A comprehensive review and emerging insights**. *Frontiers in Immunology* 2022, **13**:1010368.
11. Loyola-Rodriguez JP, Martinez-Martinez RE, Abud-Mendoza C, Patiño-Marin N, Seymour GJ: **Rheumatoid arthritis and the role of oral bacteria**. *Journal of Oral Microbiology* 2010, **2**:10.3402/jom.v3402i3400.5784.
12. Durand R, Gunselman EL, Hodges JS, Diangelis AJ, Michalowicz BS: **A pilot study of the association between cariogenic oral bacteria and preterm birth**. *Oral Dis* 2009, **15**(6):400-406.
13. Shira Davenport E: **Preterm low birthweight and the role of oral bacteria**. *J Oral Microbiol* 2010, **2**.
14. Leishman SJ, Do HL, Ford PJ: **Cardiovascular disease and the role of oral bacteria**. *J Oral Microbiol* 2010, **2**.
15. Dominy SS, Lynch C, Ermini F, Benedyk M, Marczyk A, Konradi A, Nguyen M, Haditsch U, Raha D, Griffin C *et al*: **Porphyromonas gingivalis in Alzheimer's disease brains: Evidence for disease causation and treatment with small-molecule inhibitors**. *Sci Adv* 2019, **5**(1):eaau3333.

16. Stathopoulou PG, Benakanakere MR, Galicia JC, Kinane DF: **Epithelial cell pro-inflammatory cytokine response differs across dental plaque bacterial species**. *Journal of clinical periodontology* 2010, **37**(1):24-29.
17. Di Vincenzo F, Del Gaudio A, Petito V, Lopetuso LR, Scaldaferri F: **Gut microbiota, intestinal permeability, and systemic inflammation: a narrative review**. *Intern Emerg Med* 2024, **19**(2):275-293.
18. Moreno CM, Boeree E, Freitas CMT, Weber KS: **Immunomodulatory role of oral microbiota in inflammatory diseases and allergic conditions**. *Front Allergy* 2023, **4**.
19. Chivero ET, Ahmad R, Thangaraj A, Periyasamy P, Kumar B, Kroeger E, Feng D, Guo ML, Roy S, Dhawan P *et al*: **Cocaine Induces Inflammatory Gut Milieu by Compromising the Mucosal Barrier Integrity and Altering the Gut Microbiota Colonization**. *Sci Rep* 2019, **9**(1):12187.
20. Niu F, Liao K, Hu G, Sil S, Callen S, Guo ML, Yang L, Buch S: **Cocaine-induced release of CXCL10 from pericytes regulates monocyte transmigration into the CNS**. *J Cell Biol* 2019, **218**(2):700-721.
21. Vonder Haar C, Ferland JN, Kaur S, Riparip LK, Rosi S, Winstanley CA: **Cocaine self-administration is increased after frontal traumatic brain injury and associated with neuroinflammation**. *Eur J Neurosci* 2019, **50**(3):2134-2145.
22. Fu X, Bian C, Kruyer A, Zhou Z, Luo Z, Haque A, Wagner A, Lang R, Fitting S, Robinson C *et al*: **Cocaine administration protects gut mucosa barrier and reduces plasma level of TNF-α**. *Current Psychopharmacology* 2022, **11**(2):1-8.
23. Liao K, Guo M, Niu F, Yang L, Callen SE, Buch S: **Cocaine-mediated induction of microglial activation involves the ER stress-TLR2 axis**. *J Neuroinflammation* 2016, **13**:33.
24. Pirozhkov SV, Watson RR, Chen GJ: **Ethanol enhances immunosuppression induced by cocaine**. *Alcohol* 1992, **9**(6):489-494.
25. Shen HM, Kennedy JL, Ou DW: **Inhibition of cytokine release by cocaine**. *International Journal of Immunopharmacology* 1994, **16**(4):295-300.
26. Shen HM, Sha LX, Wiederhold MD, Ou DW: **Suppression of macrophage reactive intermediates by cocaine**. *International Journal of Immunopharmacology* 1995, **17**(5):419-423.
27. Wang Y, Huang DS, Watson RR: **In vivo and in vitro cocaine modulation on production of cytokines in C57BL/6 mice**. *Life Sciences* 1994, **54**(6):401-411.
28. Fu X, Cheng D, Luo Z, Wagner A, Fitting S, Cong X, Xu W, Maas K, Wan Z, Zhu J *et al*: **Oral Enrichment of Streptococcus and its Role in Systemic Inflammation Related to Monocyte Activation in Humans with Cocaine Use Disorder**. *J Neuroimmune Pharmacol* 2021.
29. Luo Z, Li M, Wu Y, Meng Z, Martin L, Zhang L, Ogunrinde E, Zhou Z, Qin S, Wan Z *et al*: **Systemic translocation of Staphylococcus drives autoantibody production in HIV disease**. *Microbiome* 2019, **7**(1):25.
30. Luo Z, Health SL, Li M, Yang H, Wu Y, Collins M, Deeks SG, Martin JN, Scott A, Jiang W: **Variation in blood microbial lipopolysaccharide (LPS) contributes to immune reconstitution in response to suppressive antiretroviral therapy in HIV**. *EBioMedicine* 2022, **80**:104037.

31. Fultz R, Ticer T, Glover J, Stripe L, Engevik MA: **Select Streptococci Can Degrade Candida Mannan To Facilitate Growth**. *Applied and Environmental Microbiology* 2022, **88**(4):e02237-02221.
32. Krishnamurthi VR, Niyonshuti II, Chen J, Wang Y: **A new analysis method for evaluating bacterial growth with microplate readers**. *PLoS ONE* 2021, **16**(1):e0245205.
33. Lundberg P, Welander P, Han X, Cantin E: **Herpes simplex virus type 1 DNA is immunostimulatory in vitro and in vivo**. *J Virol* 2003, **77**(20):11158-11169.
34. Caselli E, Fabbri C, D'Accolti M, Soffritti I, Bassi C, Mazzacane S, Franchi M: **Defining the oral microbiome by whole-genome sequencing and resistome analysis: the complexity of the healthy picture**. *BMC Microbiology* 2020, **20**(1):120.
35. Lloyd-Price J, Mahurkar A, Rahnavard G, Crabtree J, Orvis J, Hall AB, Brady A, Creasy HH, McCracken C, Giglio MG *et al*: **Strains, functions and dynamics in the expanded Human Microbiome Project**. *Nature* 2017, **550**(7674):61-66.
36. Hime GW, Hearn WL, Rose S, Cofino J: **Analysis of cocaine and cocaethylene in blood and tissues by GC-NPD and GC-ion trap mass spectrometry**. *J Anal Toxicol* 1991, **15**(5):241-245.
37. Antoniazzi RP, Zanatta FB, Rösing CK, Feldens CA: **Association Among Periodontitis and the Use of Crack Cocaine and Other Illicit Drugs**. *Journal of Periodontology* 2016, **87**(12):1396-1405.
38. Antoniazzi RP, Sari AR, Casarin M, Moraes CMB, Feldens CA: **Association between crack cocaine use and reduced salivary flow**. *Braz Oral Res* 2017, **31**:e42.
39. Kim SG, Jung JB, Dixit D, Rovner R, Jr., Zack JA, Baldwin GC, Vatakis DN: **Cocaine exposure enhances permissiveness of quiescent T cells to HIV infection**. *J Leukoc Biol* 2013, **94**(4):835-843.
40. Napuri J, Pilakka-Kanthikeel S, Raymond A, Agudelo M, Yndart-Arias A, Saxena SK, Nair M: **Cocaine enhances HIV-1 infectivity in monocyte derived dendritic cells by suppressing microRNA-155**. *PLoS One* 2013, **8**(12):e83682.
41. Irwin MR, Olmos L, Wang M, Valladares EM, Motivala SJ, Fong T, Newton T, Butch A, Olmstead R, Cole SW: **Cocaine dependence and acute cocaine induce decreases of monocyte proinflammatory cytokine expression across the diurnal period: autonomic mechanisms**. *J Pharmacol Exp Ther* 2007, **320**(2):507-515.
42. Ersche KD, Döffinger R: **Inflammation and infection in human cocaine addiction**. *Current Opinion in Behavioral Sciences* 2017, **13**:203-209.
43. Clark KH, Wiley CA, Bradberry CW: **Psychostimulant Abuse and Neuroinflammation: Emerging Evidence of Their Interconnection**. *Neurotoxicity Research* 2013, **23**(2):174-188.
44. Thomas DM, Walker PD, Benjamins JA, Geddes TJ, Kuhn DM: **Methamphetamine neurotoxicity in dopamine nerve endings of the striatum is associated with microglial activation**. *The Journal of Pharmacology and Experimental Therapeutics* 2004, **311**(1):1-7.
45. Gao Y, Kong D, Sun J-x, Ma Z-x, Wang G-q, Ma X-f, Sun L, Luo H-y, Xu Y, Wang K-h: **Intestinal barrier damage caused by addictive substance use disorder**. *European Journal of Medical Research* 2025, **30**(1):226.

46. Volpe GE, Ward H, Mwamburi M, Dinh D, Bhalchandra S, Wanke C, Kane AV: **Associations of cocaine use and HIV infection with the intestinal microbiota, microbial translocation, and inflammation**. *J Stud Alcohol Drugs* 2014, **75**(2):347-357.
47. Davidson TL, Hargrave SL, Kearns DN, Clasen MM, Jones S, Wakeford AGP, Sample CH, Riley AL: **Cocaine impairs serial-feature negative learning and blood-brain barrier integrity**. *Pharmacol Biochem Behav* 2018, **170**:56-63.
48. Chen Q, Wu G, Chen H, Li H, Li S, Zhang C, Pang X, Wang L, Zhao L, Shen J: **Quantification of Human Oral and Fecal Streptococcus parasanguinis by Use of Quantitative Real-Time PCR Targeting the groEL Gene**. *Front Microbiol* 2019, **10**:2910.
49. Patrakka O, Pienimaki JP, Tuomisto S, Ollikainen J, Lehtimaki T, Karhunen PJ, Martiskainen M: **Oral Bacterial Signatures in Cerebral Thrombi of Patients With Acute Ischemic Stroke Treated With Thrombectomy**. *J Am Heart Assoc* 2019, **8**(11):e012330.
50. Dasanayake AP, Li Y, Wiener H, Ruby JD, Lee MJ: **Salivary Actinomyces naeslundii genospecies 2 and Lactobacillus casei levels predict pregnancy outcomes**. *J Periodontol* 2005, **76**(2):171-177.
51. Marsh PD, Moter A, Devine DA: **Dental plaque biofilms: communities, conflict and control**. *Periodontology 2000* 2011, **55**(1):16-35.
52. Nicholson JS, Landry KS: **Oral Dysbiosis and Neurodegenerative Diseases: Correlations and Potential Causations**. *Microorganisms* 2022, **10**(7):1326.
53. Sampaio-Maia B, Caldas IM, Pereira ML, Pérez-Mongiovi D, Araujo R: **The Oral Microbiome in Health and Its Implication in Oral and Systemic Diseases**. *Adv Appl Microbiol* 2016, **97**:171-210.
54. Shrimali T, Malhotra S, Relhan N, Tak V, Choudhary SK, Gupta N, Singh AK: **Streptococcus parasanguinis: An emerging pathogen causing neonatal endocarditis: A case report**. *Access Microbiology* 2023, **5**(6):000576.v000574.
55. Cugini C, Shanmugam M, Landge N, Ramasubbu N: **The Role of Exopolysaccharides in Oral Biofilms**. *Journal of Dental Research* 2019, **98**(7):739-745.
56. Abranches J, Zeng L, Kajfasz JK, Palmer SR, Chakraborty B, Wen ZT, Richards VP, Brady LJ, Lemos JA: **Biology of Oral Streptococci**. *Microbiol Spectr* 2018, **6**(5).
57. Hajishengallis G: **Periodontitis: from microbial immune subversion to systemic inflammation**. *Nature reviews Immunology* 2015, **15**(1):30.
58. Kebschull M, Demmer RT, Papapanou PN: **"Gum Bug, Leave My Heart Alone!"—Epidemiologic and Mechanistic Evidence Linking Periodontal Infections and Atherosclerosis**. *Journal of Dental Research* 2010, **89**(9):879-902.
59. Chen Q, Sun B, Wu H, Peng Z, Fives-Taylor PM: **Differential roles of individual domains in selection of secretion route of a Streptococcus parasanguinis serine-rich adhesin, Fap1**. *Journal of Bacteriology* 2007, **189**(21):7610-7617.
60. Ascenzi P, Clementi E, Polticelli F: **The Rhodococcus sp. cocaine esterase: a bacterial candidate for novel pharmacokinetic-based therapies for cocaine abuse**. *IUBMB life* 2003, **55**(7):397-402.
61. Potruch A, Schwartz A, Ilan Y: **The role of bacterial translocation in sepsis: a new target for therapy**. *Therap Adv Gastroenterol* 2022, **15**:17562848221094214.

62. Gnauck A, Lentle RG, Kruger MC: **The Characteristics and Function of Bacterial Lipopolysaccharides and Their Endotoxic Potential in Humans**. *Int Rev Immunol* 2016, **35**(3):189-218.
63. Potrykus M, Czaja-Stolc S, Stankiewicz M, Kaska Ł, Małgorzewicz S: **Intestinal Microbiota as a Contributor to Chronic Inflammation and Its Potential Modifications**. *Nutrients* 2021, **13**(11):3839.
64. Pelletier LL: **Microbiology of the Circulatory System**. In: *Medical Microbiology.* Edited by Baron S, 4th edn. Galveston (TX): University of Texas Medical Branch at Galveston; 1996.
65. Zimmerman JL: **Cocaine intoxication**. *Crit Care Clin* 2012, **28**(4):517-526.

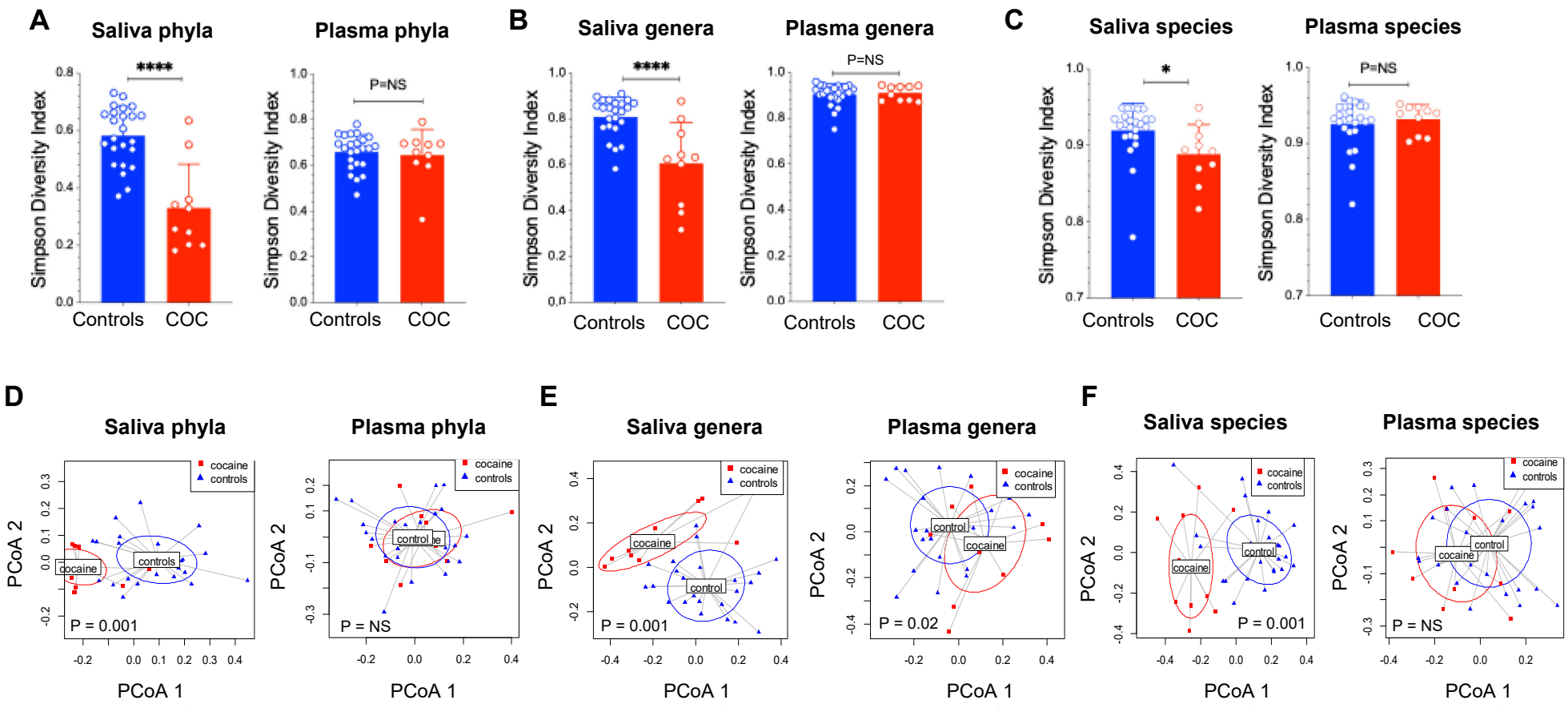
A
Saliva phyla
Plasma phyla
B
Saliva genera
Plasma genera
C
Saliva species
Plasma species
Simpson Diversity Index
****
P=NS
*
Controls
COC
D
E
F
PCoA 1
PCoA 2
cocaine
controls
control
P = 0.001
P = NS
P = 0.02

Figure 1

A

Saliva and plasma relative abundance in genera (log2)

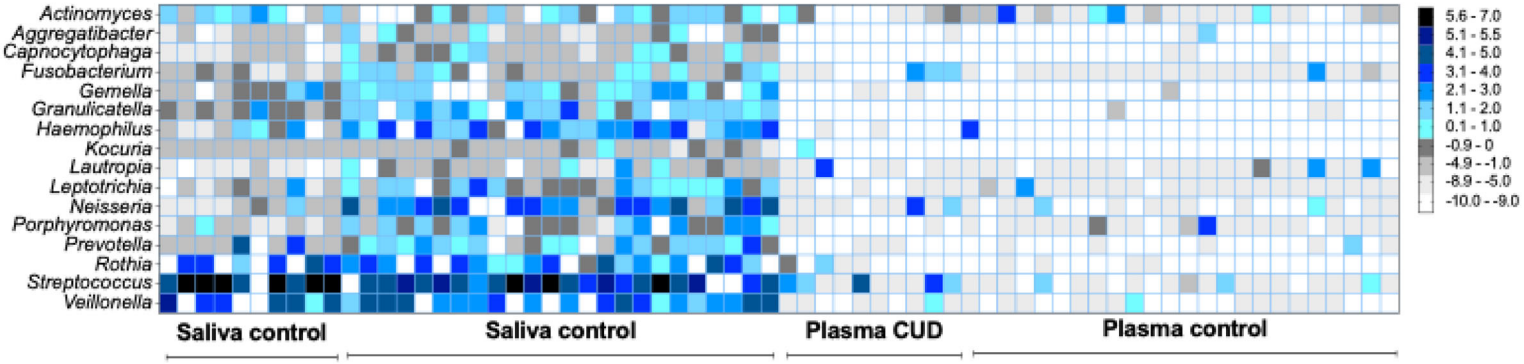

Saliva genus abundance (log2)

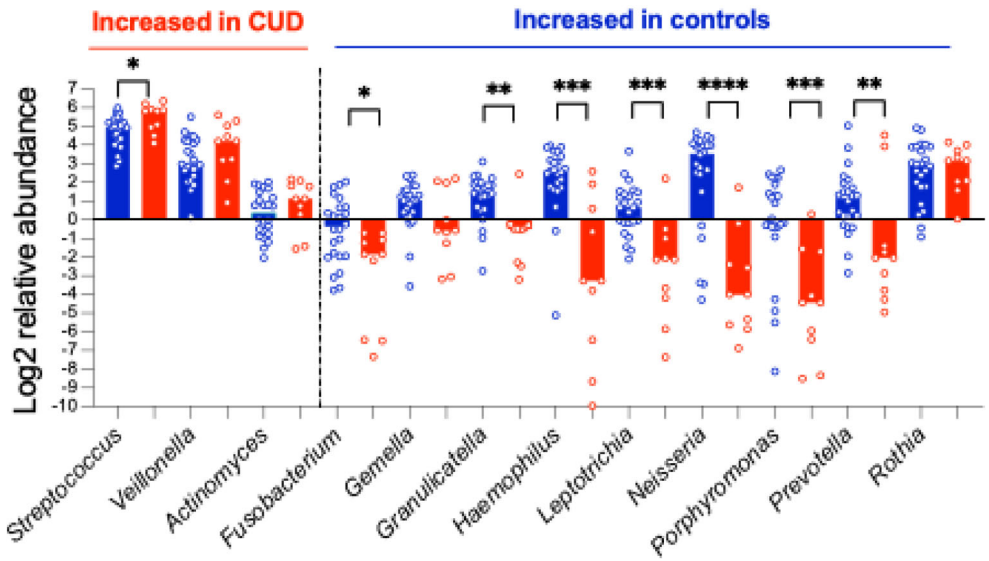

Plasma genus abundance (%)

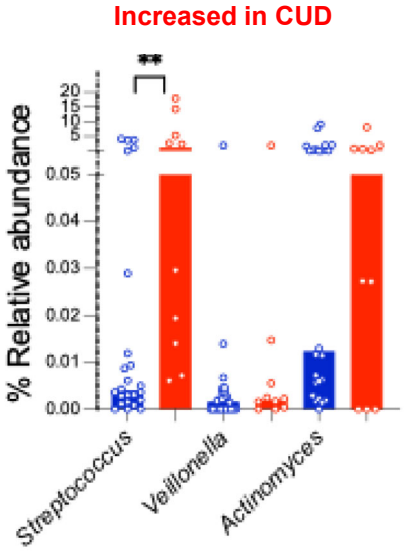

Figure 2A

B

Saliva and plasma relative abundance in species (log2)

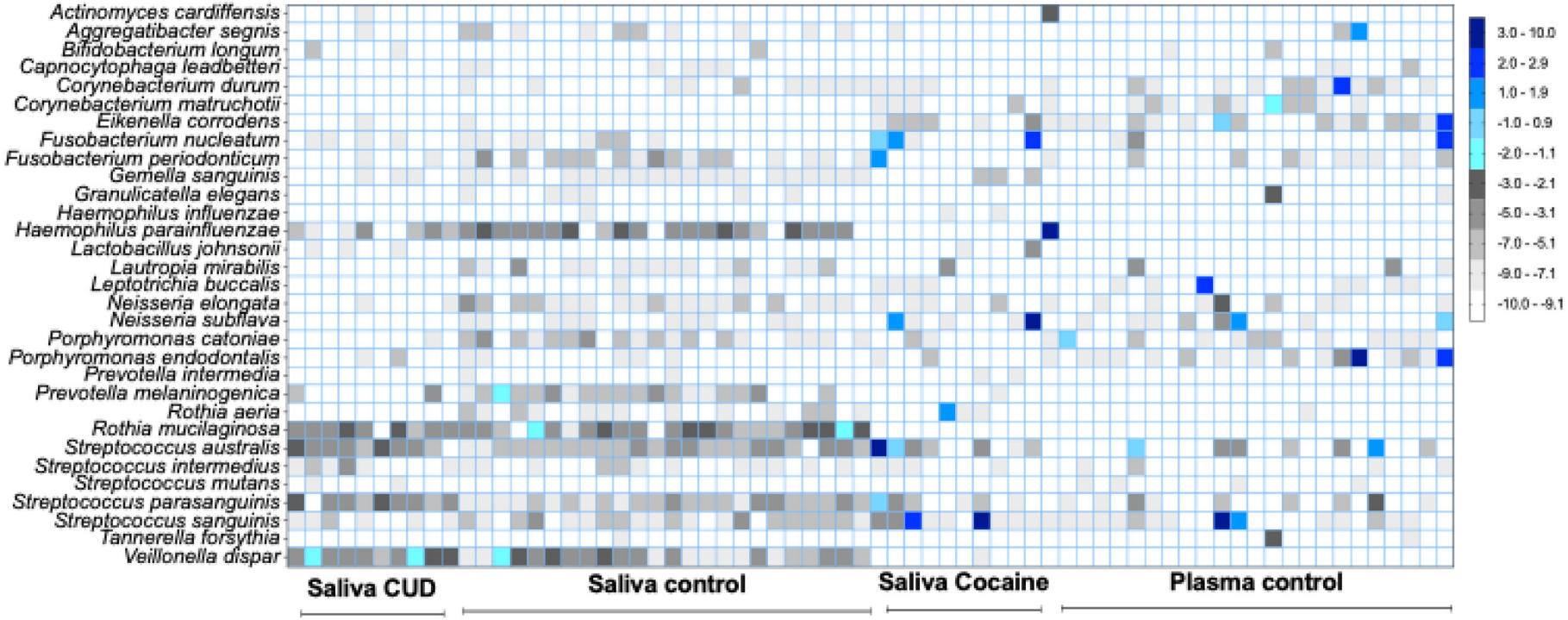

Figure 2B

Saliva species abundance

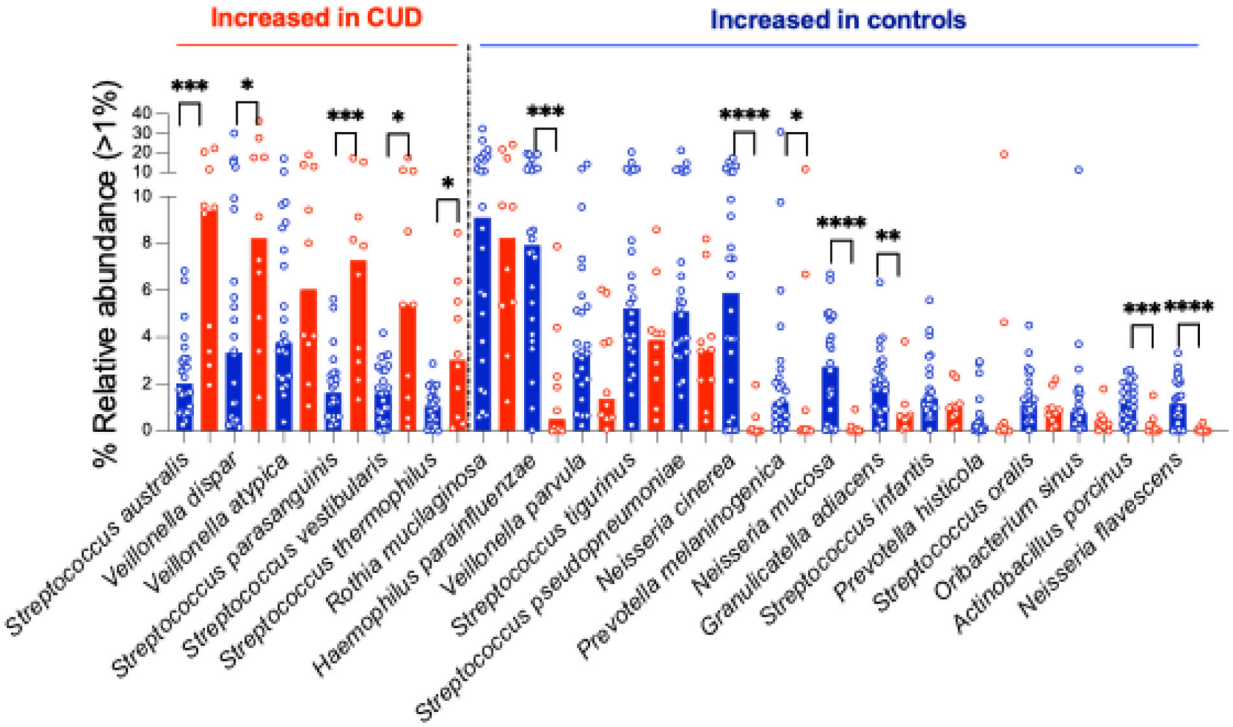

Plasma species abundance

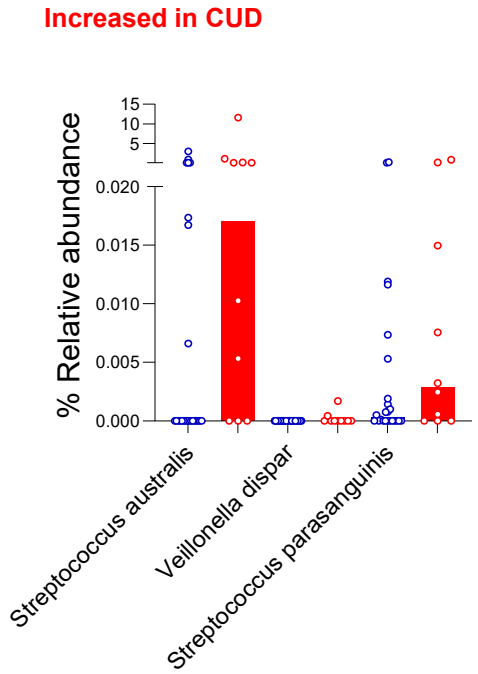

Figure 2B

C

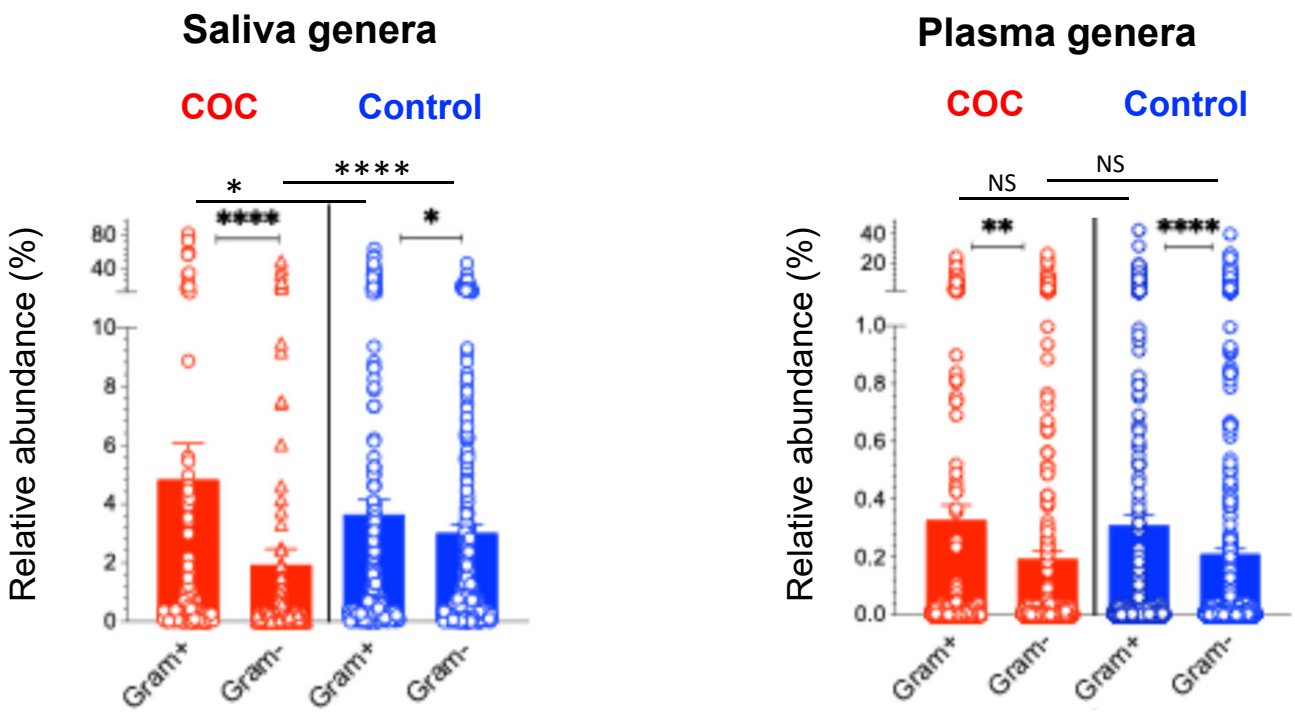
Saliva genera
COC
Control
Relative abundance (%)
80
40
10
8
6
4
2
0
*
****
****
*
Gram+
Gram-
Gram+
Gram-
Plasma genera
COC
Control
Relative abundance (%)
40
20
1.0
0.8
0.6
0.4
0.2
0.0
NS
NS
**
****
Gram+
Gram-
Gram+
Gram-

Figure 2C

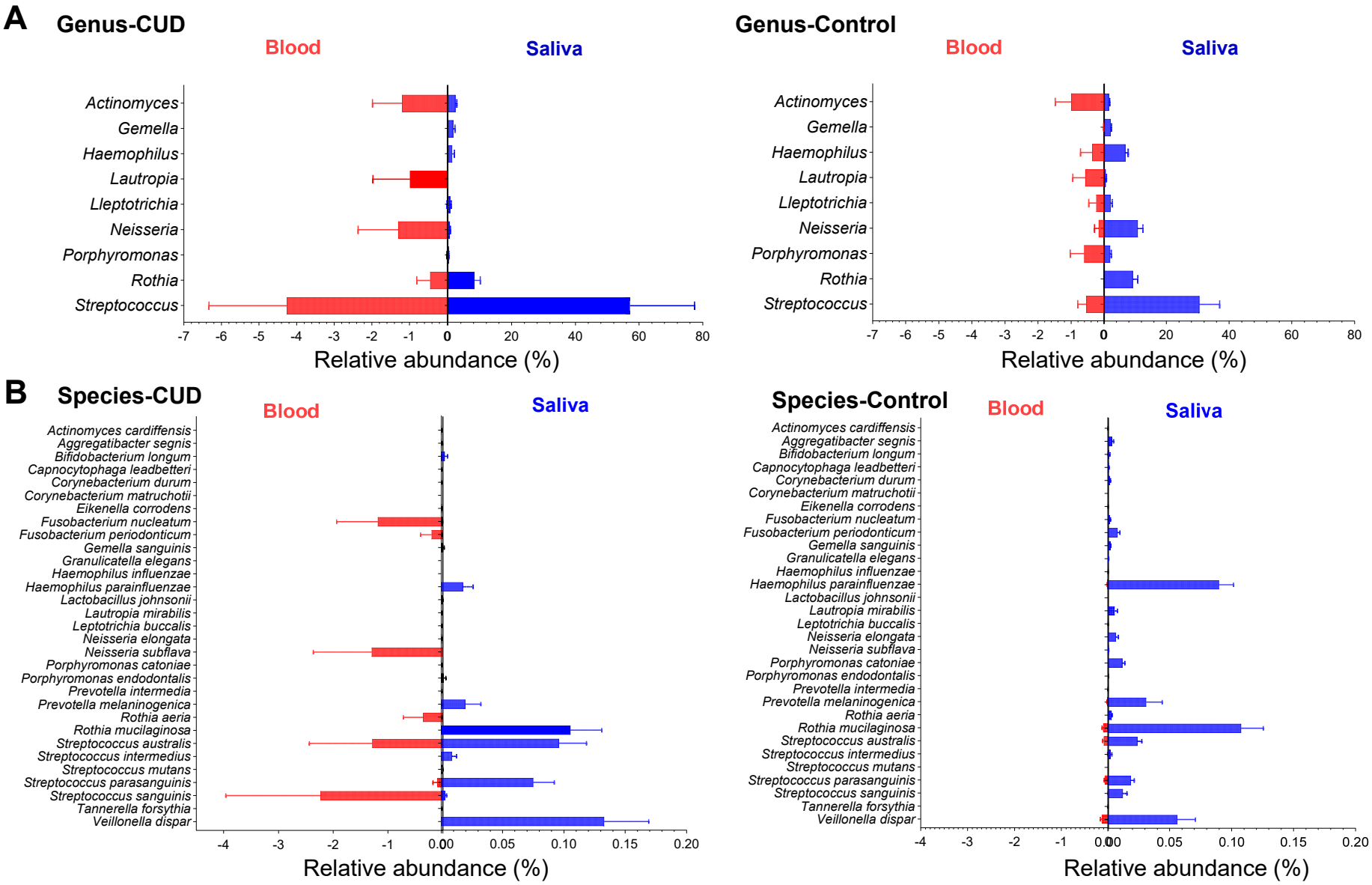
A
Genus-CUD
Blood
Saliva
Actinomyces
Gemella
Haemophilus
Lautropia
Lleptotrichia
Neisseria
Porphyromonas
Rothia
Streptococcus
-7 -6 -5 -4 -3 -2 -1 0 20 40 60 80
Relative abundance (%)
Genus-Control
Blood
Saliva
Actinomyces
Gemella
Haemophilus
Lautropia
Lleptotrichia
Neisseria
Porphyromonas
Rothia
Streptococcus
-7 -6 -5 -4 -3 -2 -1 0 20 40 60 80
Relative abundance (%)
B
Species-CUD
Blood
Saliva
Actinomyces cardiffensis
Aggregatibacter segnis
Bifidobacterium longum
Capnocytophaga leadbetteri
Corynebacterium durum
Corynebacterium matruchotii
Eikenella corrodens
Fusobacterium nucleatum
Fusobacterium periodonticum
Gemella sanguinis
Granulicatella elegans
Haemophilus influenzae
Haemophilus parainfluenzae
Lactobacillus johnsonii
Lautropia mirabilis
Leptotrichia buccalis
Neisseria elongata
Neisseria subflava
Porphyromonas catoniae
Porphyromonas endodontalis
Prevotella intermedia
Prevotella melaninogenica
Rothia aeria
Rothia mucilaginosa
Streptococcus australis
Streptococcus intermedius
Streptococcus mutans
Streptococcus parasanguinis
Streptococcus sanguinis
Tannerella forsythia
Veillonella dispar
-4 -3 -2 -1 0.00 0.05 0.10 0.15 0.20
Relative abundance (%)
Species-Control
Blood
Saliva
Actinomyces cardiffensis
Aggregatibacter segnis
Bifidobacterium longum
Capnocytophaga leadbetteri
Corynebacterium durum
Corynebacterium matruchotii
Eikenella corrodens
Fusobacterium nucleatum
Fusobacterium periodonticum
Gemella sanguinis
Granulicatella elegans
Haemophilus influenzae
Haemophilus parainfluenzae
Lactobacillus johnsonii
Lautropia mirabilis
Leptotrichia buccalis
Neisseria elongata
Neisseria subflava
Porphyromonas catoniae
Porphyromonas endodontalis
Prevotella intermedia
Prevotella melaninogenica
Rothia aeria
Rothia mucilaginosa
Streptococcus australis
Streptococcus intermedius
Streptococcus mutans
Streptococcus parasanguinis
Streptococcus sanguinis
Tannerella forsythia
Veillonella dispar
-4 -3 -2 -1 0.00 0.05 0.10 0.15 0.20
Relative abundance (%)

Figure 3

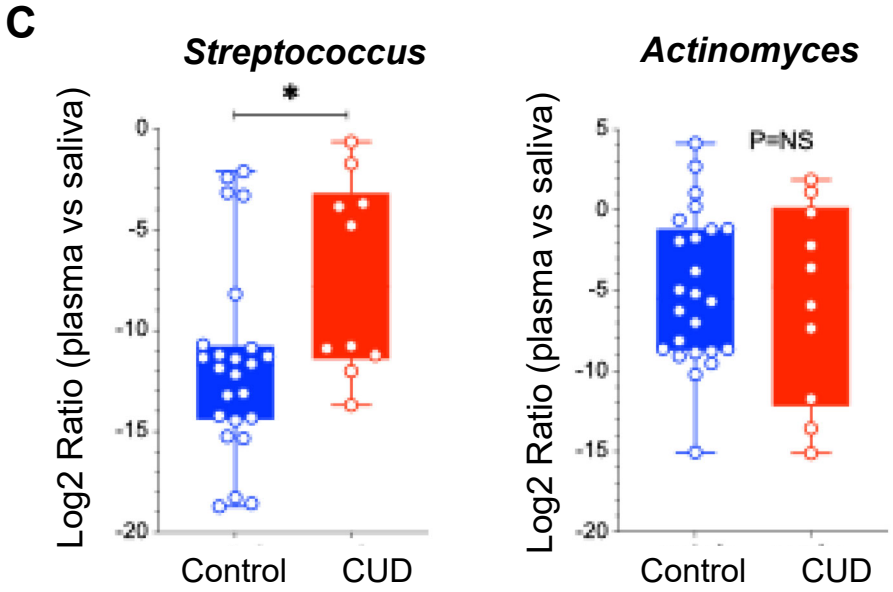
C
Streptococcus
Actinomyces
Log2 Ratio (plasma vs saliva)
Log2 Ratio (plasma vs saliva)
*
P=NS
0
-5
-10
-15
-20
5
0
-5
-10
-15
-20
Control
CUD
Control
CUD

Figure 3

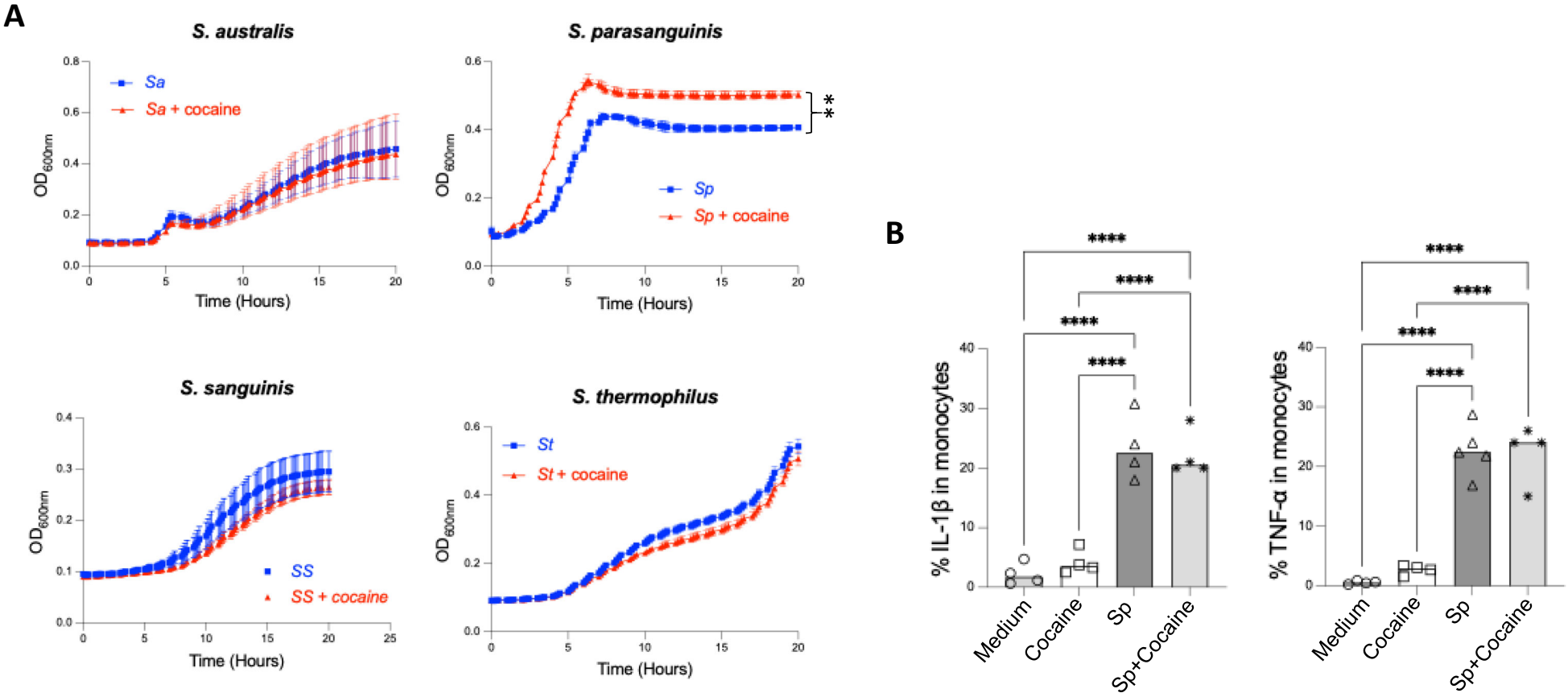
A
S. australis
Sa
Sa + cocaine
OD600nm
Time (Hours)
S. parasanguinis
Sp
Sp + cocaine
**
S. sanguinis
SS
SS + cocaine
S. thermophilus
St
St + cocaine
B
% IL-1β in monocytes
% TNF-α in monocytes
****
*
Medium
Cocaine
Sp
Sp+Cocaine

Figure 4

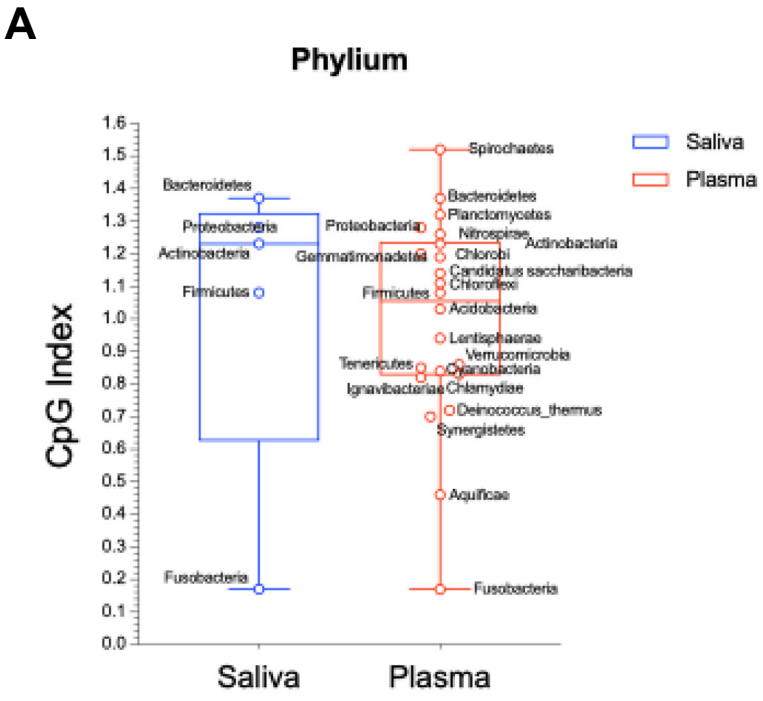
A
Phylium
CpG Index
1.6
1.5
1.4
1.3
1.2
1.1
1.0
0.9
0.8
0.7
0.6
0.5
0.4
0.3
0.2
0.1
0.0
Saliva
Plasma
Bacteroidetes
Proteobacteria
Actinobacteria
Firmicutes
Fusobacteria
Spirochaetes
Bacteroidetes
Planctomycetes
Nitrospirae
Actinobacteria
Chlorobi
Candidatus saccharibacteria
Chloroflexi
Proteobacteria
Gammatimonadetes
Firmicutes
Acidobacteria
Lentisphaerae
Verrucomicrobia
Tenericutes
Cyanobacteria
Ignavibacteriae
Chlamydiae
Deinococcus_thermus
Synergistetes
Aquificae
Fusobacteria

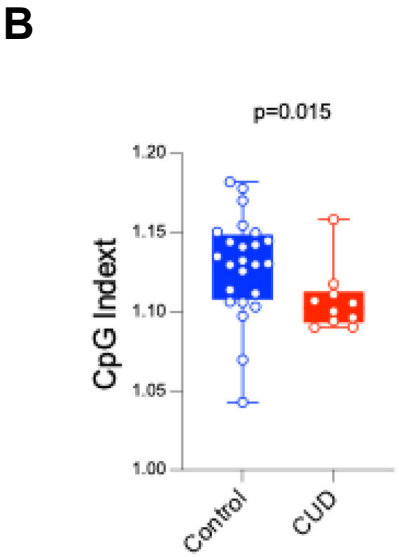
B
p=0.015
CpG Indext
1.20
1.15
1.10
1.05
1.00
Control
CUD

Figure 5

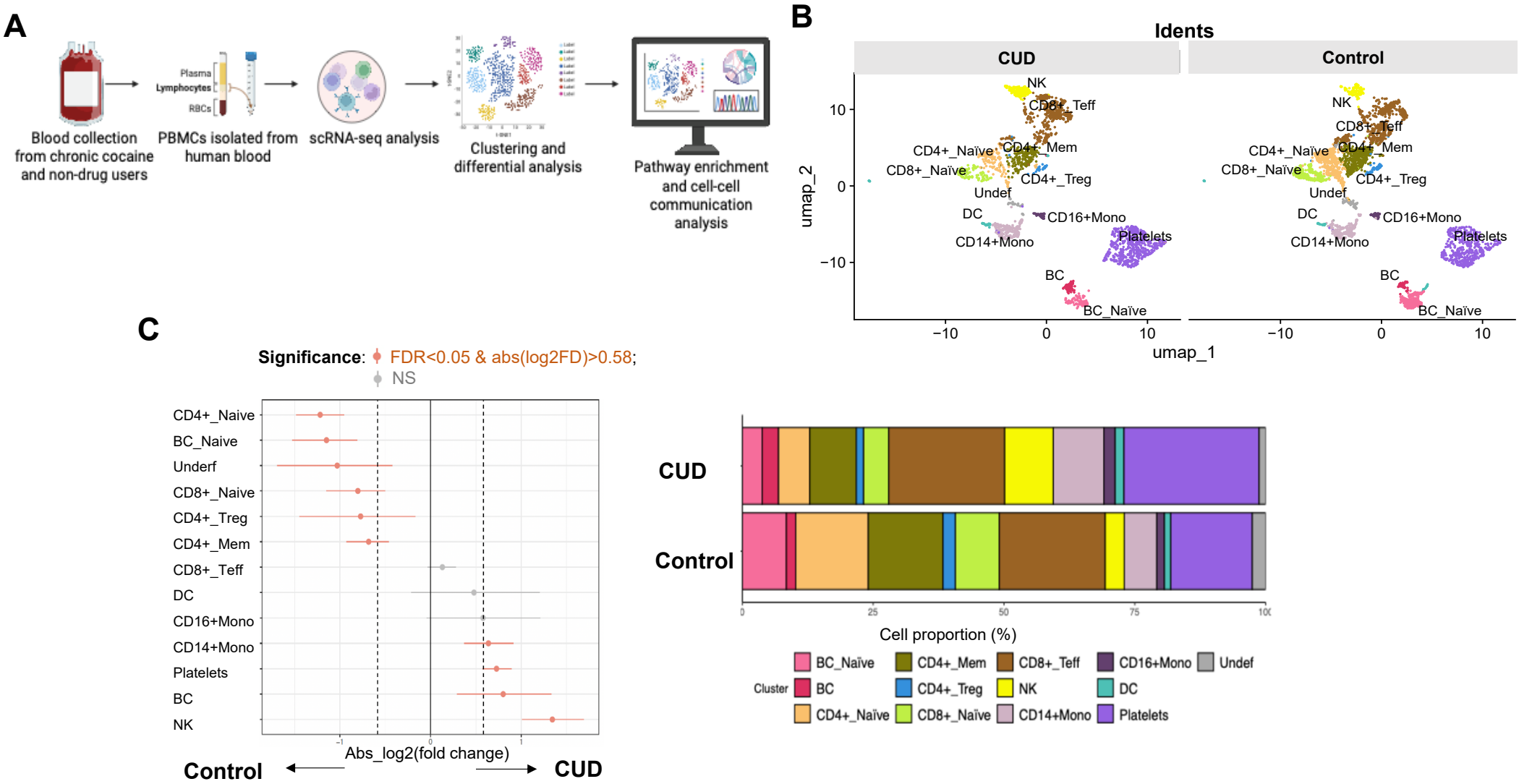
A
Blood collection from chronic cocaine and non-drug users
Plasma
Lymphocytes
RBCs
PBMCs isolated from human blood
scRNA-seq analysis
Clustering and differential analysis
Pathway enrichment and cell-cell communication analysis
B
Idents
CUD
Control
NK
CD8+_Teff
CD4+_Naïve
CD4+_Mem
CD8+_Naïve
CD4+_Treg
Undef
DC
CD16+Mono
CD14+Mono
Platelets
BC
BC_Naïve
umap_2
umap_1
C
Significance: FDR<0.05 & abs(log2FD)>0.58; NS
CD4+_Naive
BC_Naive
Underf
CD8+_Naive
CD4+_Treg
CD4+_Mem
CD8+_Teff
DC
CD16+Mono
CD14+Mono
Platelets
BC
NK
Abs_log2(fold change)
Control
CUD
Cell proportion (%)
Cluster
BC_Naïve
BC
CD4+_Naïve
CD4+_Mem
CD4+_Treg
CD8+_Naïve
CD8+_Teff
NK
CD14+Mono
CD16+Mono
DC
Platelets
Undef

Figure 6

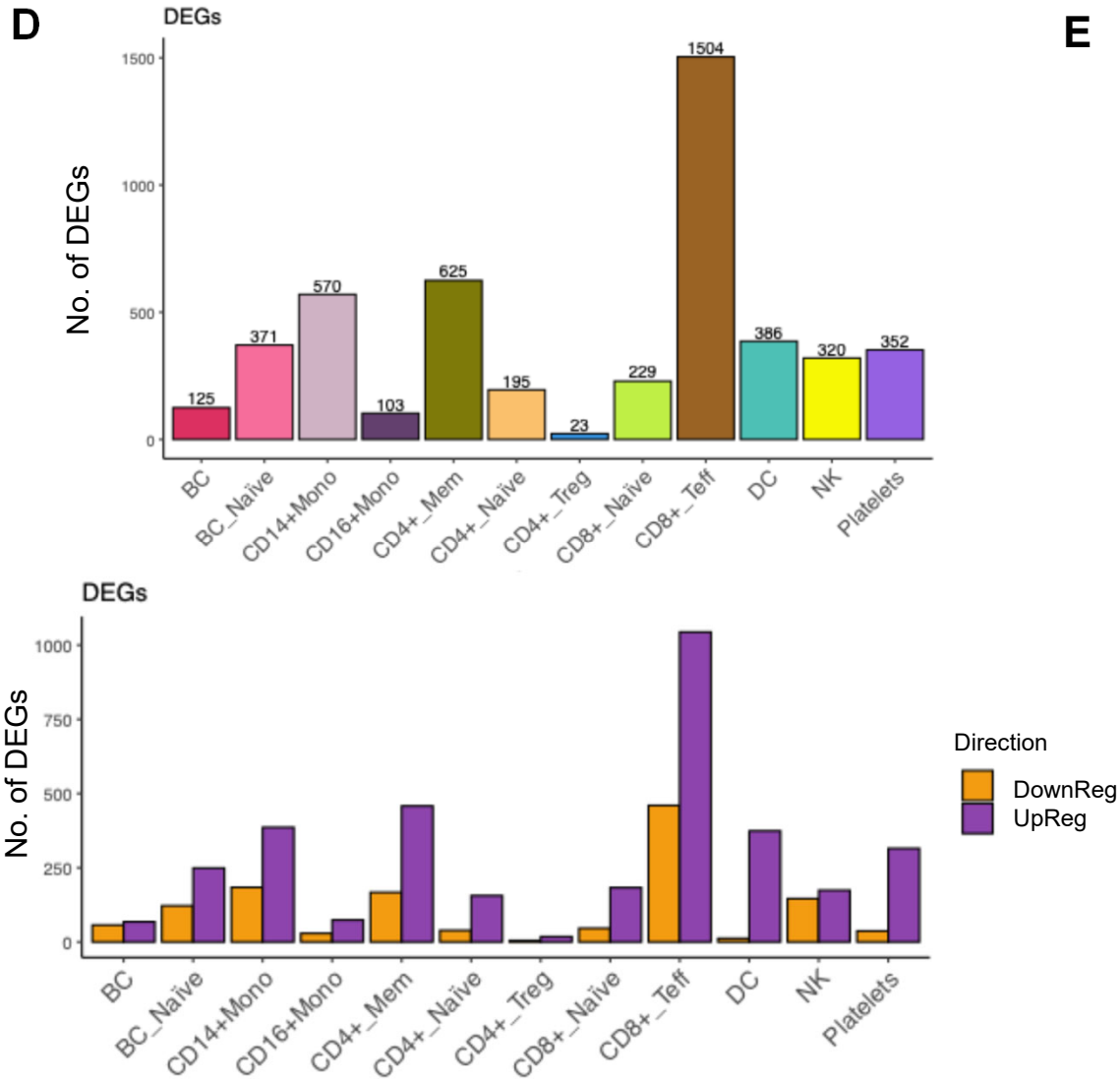
D
DEGs
No. of DEGs
1500
1000
500
0
125
371
570
103
625
195
23
229
1504
386
320
352
BC
BC_Naïve
CD14+Mono
CD16+Mono
CD4+_Mem
CD4+_Naïve
CD4+_Treg
CD8+_Naïve
CD8+_Teff
DC
NK
Platelets
DEGs
No. of DEGs
1000
750
500
250
0
Direction
DownReg
UpReg

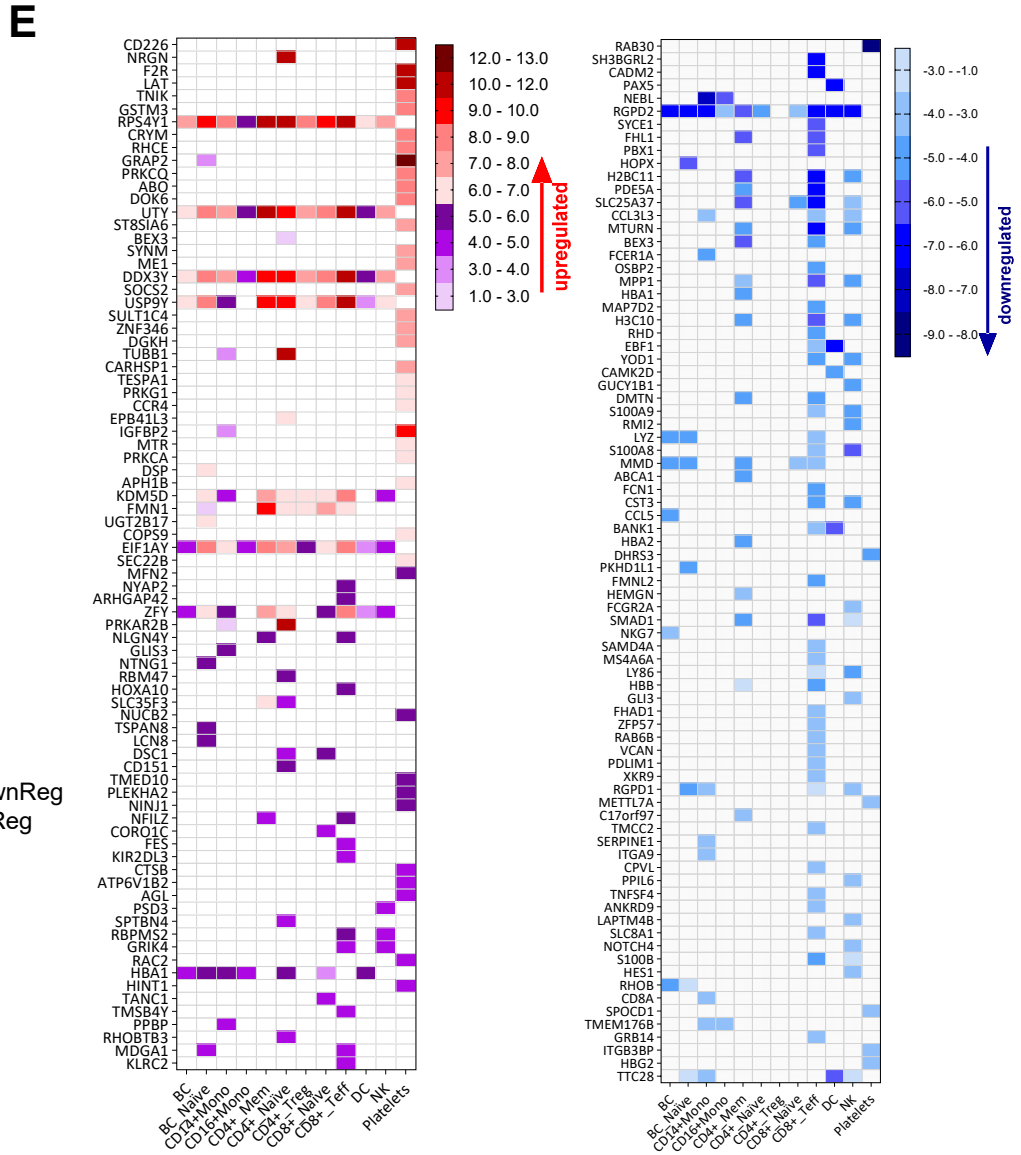
E
12.0 - 13.0
10.0 - 12.0
9.0 - 10.0
8.0 - 9.0
7.0 - 8.0
6.0 - 7.0
5.0 - 6.0
4.0 - 5.0
3.0 - 4.0
1.0 - 3.0
upregulated
-3.0 - -1.0
-4.0 - -3.0
-5.0 - -4.0
-6.0 - -5.0
-7.0 - -6.0
-8.0 - -7.0
-9.0 - -8.0
downregulated
BC
BC_Naïve
CD14+Mono
CD16+Mono
CD4+_Mem
CD4+_Naïve
CD4+_Treg
CD8+_Naïve
CD8+_Teff
DC
NK
Platelets

Figure 6

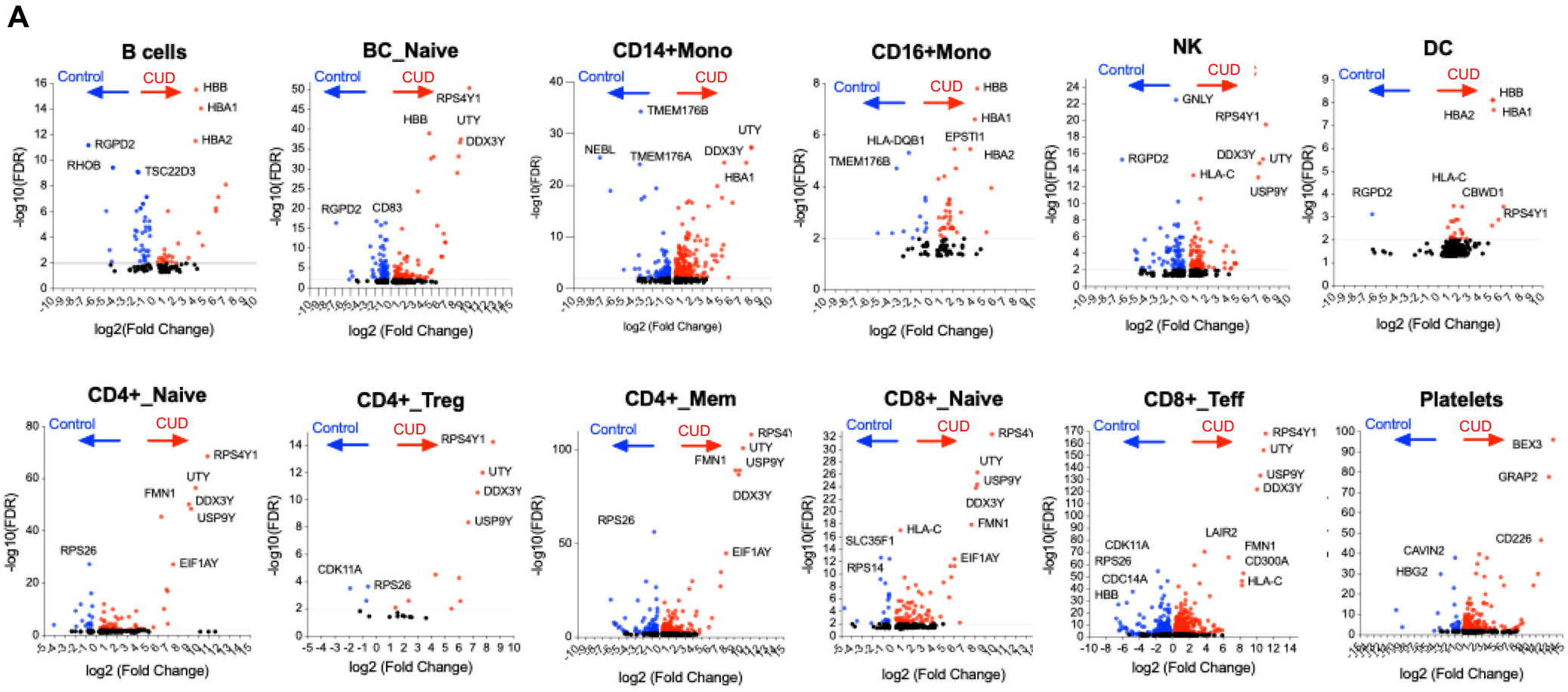
A
B cells
Control
CUD
HBB
HBA1
HBA2
RGPD2
RHOB
TSC22D3
-log10(FDR)
log2(Fold Change)
BC_Naive
RPS4Y1
HBB
UTY
DDX3Y
RGPD2
CD83
log2 (Fold Change)
CD14+Mono
TMEM176B
UTY
NEBL
TMEM176A
DDX3Y
HBA1
CD16+Mono
HBB
HBA1
HLA-DQB1
EPSTI1
TMEM176B
HBA2
NK
GNLY
RPS4Y1
RGPD2
DDX3Y
UTY
HLA-C
USP9Y
DC
HBB
HBA2
HBA1
HLA-C
RGPD2
CBWD1
RPS4Y1
CD4+_Naive
RPS4Y1
UTY
FMN1
DDX3Y
USP9Y
RPS26
EIF1AY
CD4+_Treg
RPS4Y1
UTY
DDX3Y
USP9Y
CDK11A
RPS26
CD4+_Mem
RPS4Y
UTY
FMN1
USP9Y
DDX3Y
RPS26
EIF1AY
CD8+_Naive
RPS4Y
UTY
USP9Y
DDX3Y
FMN1
HLA-C
SLC35F1
EIF1AY
RPS14
CD8+_Teff
RPS4Y1
UTY
USP9Y
DDX3Y
LAIR2
CDK11A
FMN1
RPS26
CD300A
CDC14A
HLA-C
HBB
Platelets
BEX3
GRAP2
CD226
CAVIN2
HBG2

Figure 7A

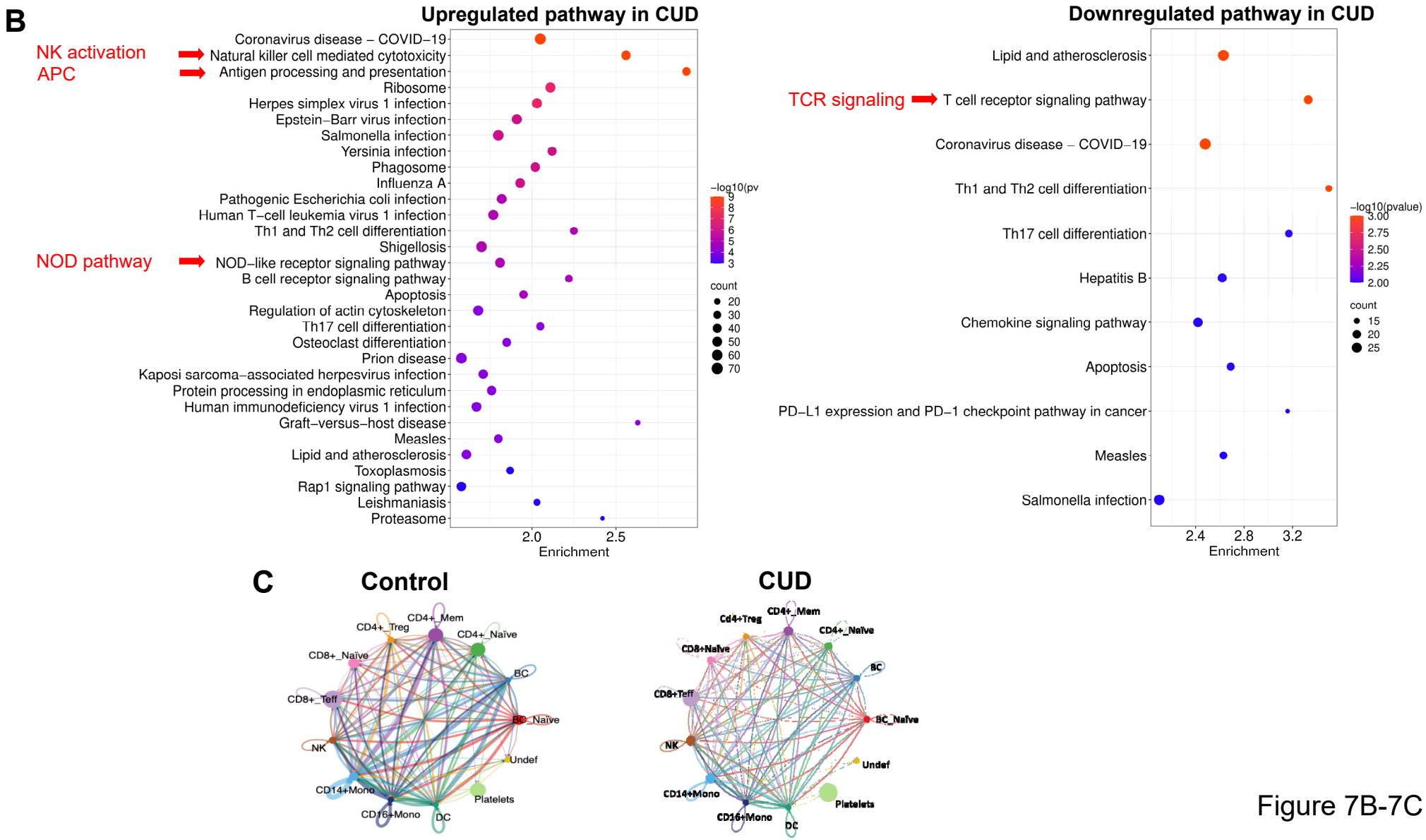
B
Upregulated pathway in CUD
NK activation
APC
NOD pathway
Coronavirus disease – COVID–19
Natural killer cell mediated cytotoxicity
Antigen processing and presentation
Ribosome
Herpes simplex virus 1 infection
Epstein–Barr virus infection
Salmonella infection
Yersinia infection
Phagosome
Influenza A
Pathogenic Escherichia coli infection
Human T–cell leukemia virus 1 infection
Th1 and Th2 cell differentiation
Shigellosis
NOD–like receptor signaling pathway
B cell receptor signaling pathway
Apoptosis
Regulation of actin cytoskeleton
Th17 cell differentiation
Osteoclast differentiation
Prion disease
Kaposi sarcoma–associated herpesvirus infection
Protein processing in endoplasmic reticulum
Human immunodeficiency virus 1 infection
Graft–versus–host disease
Measles
Lipid and atherosclerosis
Toxoplasmosis
Rap1 signaling pathway
Leishmaniasis
Proteasome
2.0
2.5
Enrichment
–log10(pv
9
8
7
6
5
4
3
count
20
30
40
50
60
70
Downregulated pathway in CUD
TCR signaling
Lipid and atherosclerosis
T cell receptor signaling pathway
Coronavirus disease – COVID–19
Th1 and Th2 cell differentiation
Th17 cell differentiation
Hepatitis B
Chemokine signaling pathway
Apoptosis
PD–L1 expression and PD–1 checkpoint pathway in cancer
Measles
Salmonella infection
2.4
2.8
3.2
Enrichment
–log10(pvalue)
3.00
2.75
2.50
2.25
2.00
count
15
20
25
C
Control
CD4+_Mem
CD4+_Treg
CD4+_Naïve
CD8+_Naïve
BC
CD8+_Teff
BC_Naïve
NK
Undef
CD14+Mono
Platelets
CD16+Mono
DC
CUD
CD4+_Mem
Cd4+Treg
CD4+_Naïve
CD8+Naïve
BC
CD8+Teff
BC_Naïve
NK
Undef
CD14+Mono
Platelets
CD16+Mono
DC

Figure 7B-7C

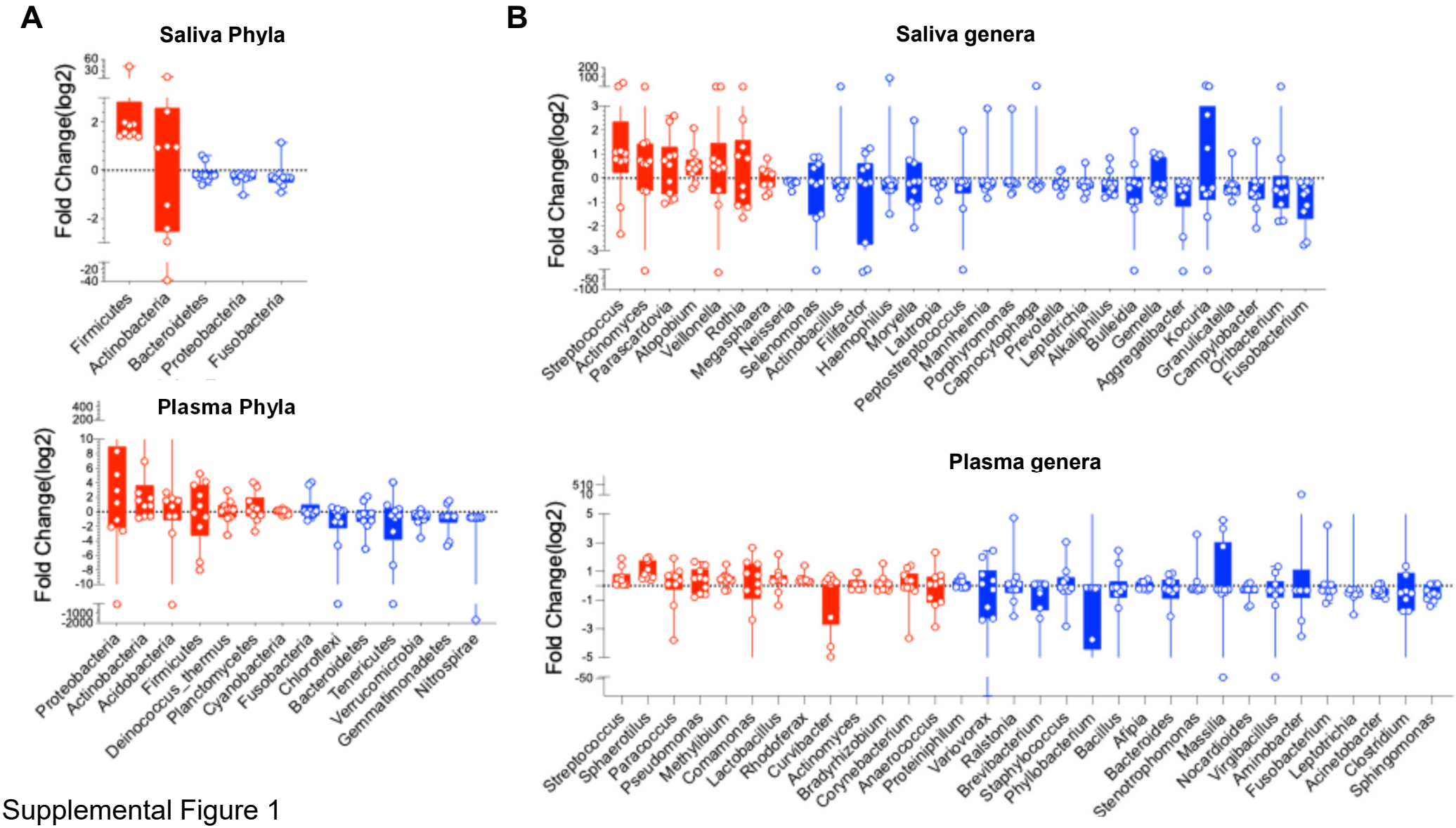

Supplemental Figure 1

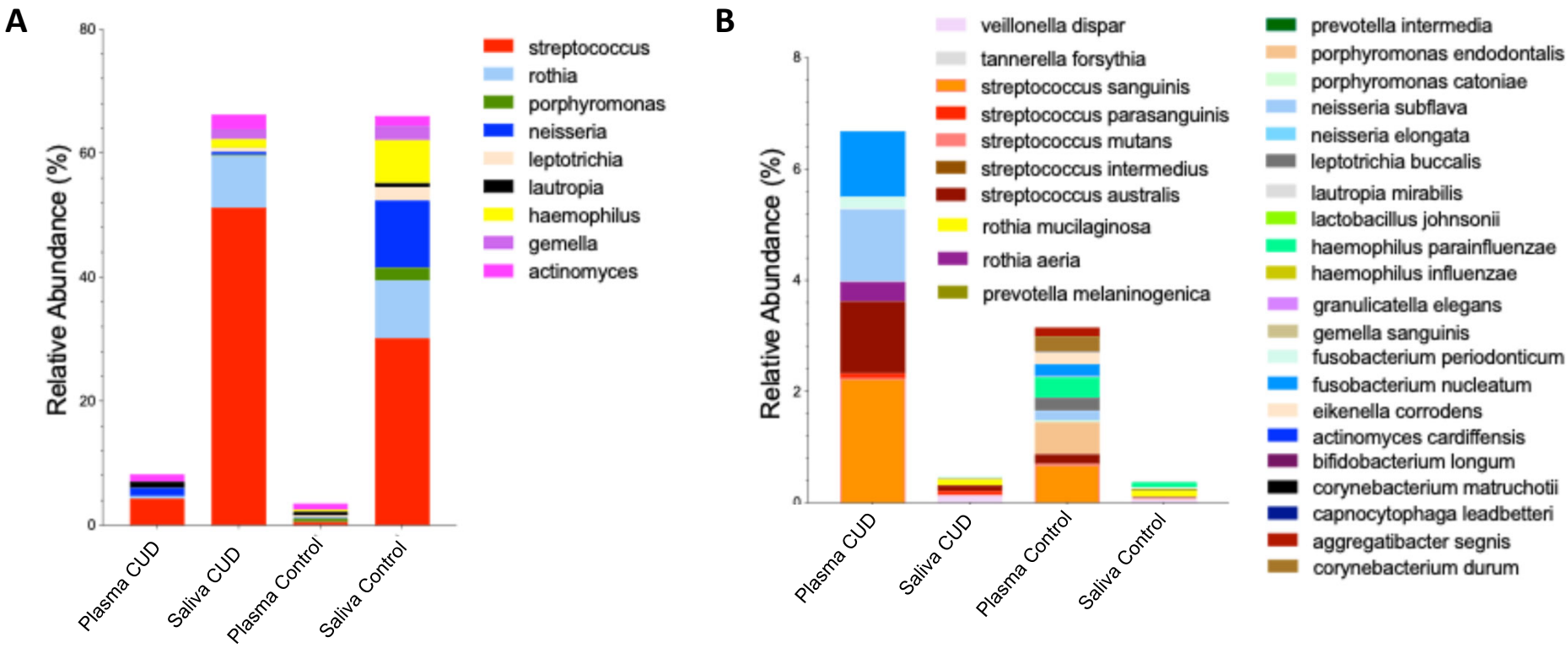

Supplemental Figure 2

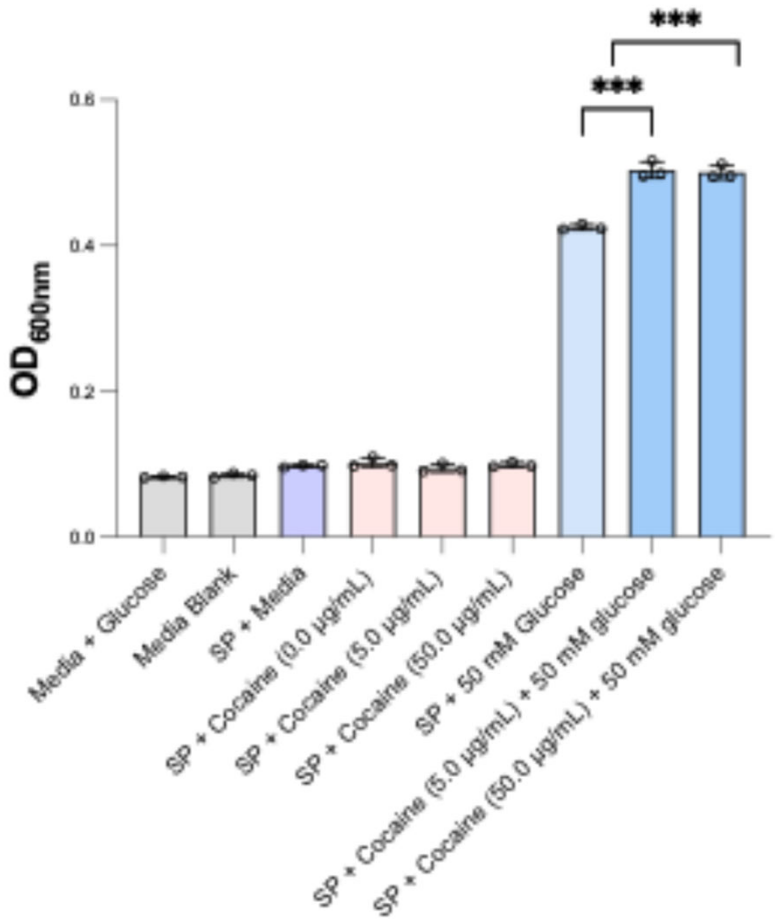

Supplemental Figure 3

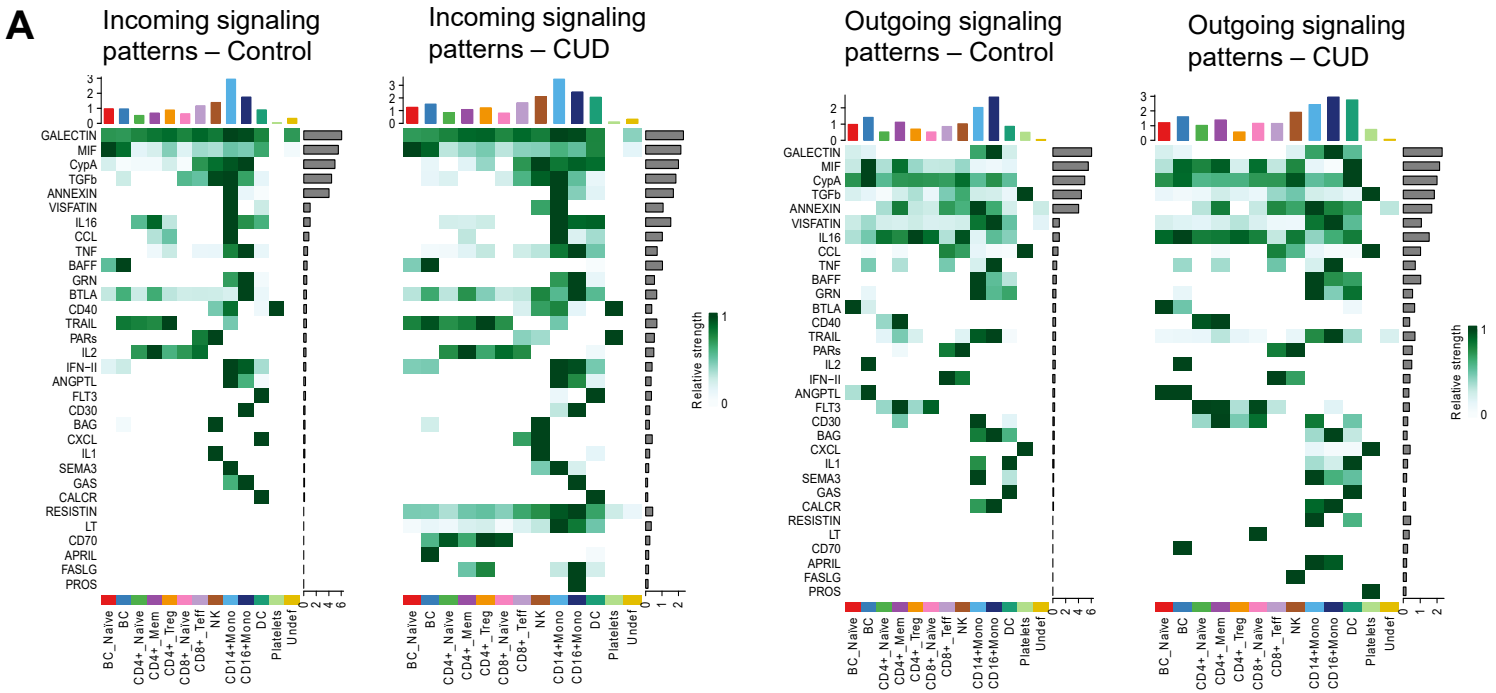

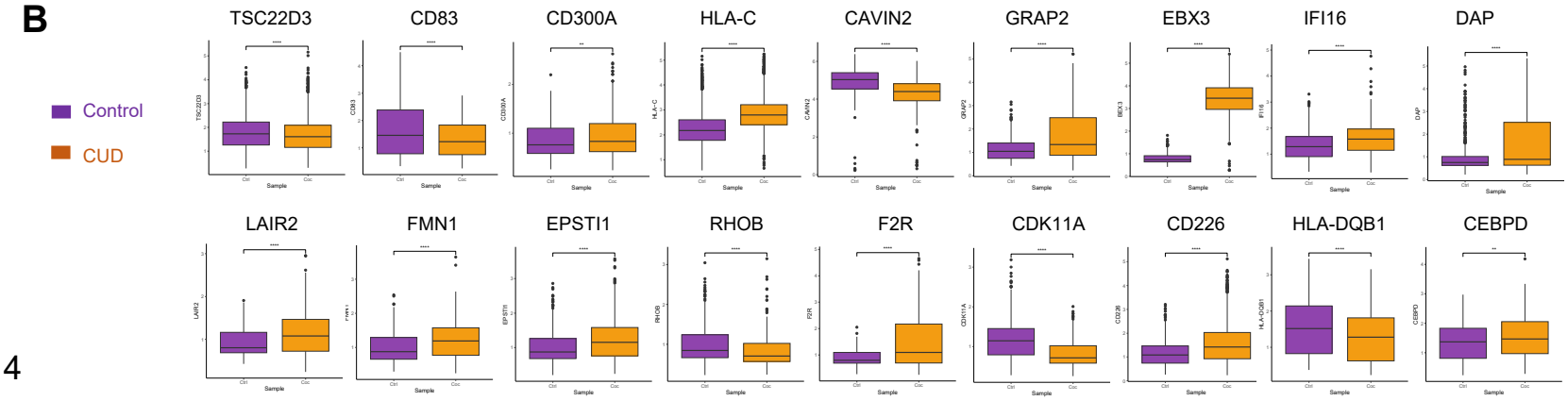

Supplemental Figure 4